# A DISULFIDE-BONDED DIMER OF THE CORE PROTEIN OF HEPATITIS C VIRUS IS IMPORTANT FOR VIRUS-LIKE PARTICLE PRODUCTION

**Yukihiro Kushima,[1, 2] Takaji Wakita,[3] Makoto Hijikata[1, 2, *]**

1. **Department of Viral Oncology, Institute for Virus Research, Kyoto University, Kyoto 606-8507, Japan**
2. **Graduate School of Biostudies, Kyoto University, Kyoto 606-8507, Japan**
3. **Department of Virology II, National Institute of Infectious Diseases, Tokyo 162-8640, Japan**

***Corresponding author**

**Tel: +81-75-751-4046**

**Fax: +81-75-751-3998**

**email: mhijikat@virus.kyoto-u.ac.jp**

word count:

abstract; 209 words

text; 4987 words

**ABSTRACT**

Hepatitis C virus (HCV) core protein forms the nucleocapsid of the HCV particle. Although many functions of core protein have been reported, how the HCV particle is assembled is not well understood. Here we show that the nucelocapsid-like particle of HCV is composed of a disulfide-bonded core complex (dbc-complex). We also found that the disulfide-bonded dimer of the core (dbd-core) is formed at the endoplasmic reticulum (ER) where the core protein is initially produced and processed. Mutational analysis revealed that the cysteine residue at amino-acid position 128 (Cys128) of the core, a highly conserved residues among almost all reported isolates, is responsible for dbd-core formation and virus-like particle production with no effect on the replication of HCV RNA genome and the several known functions of the core, including RNA binding ability and localization to the lipid droplet. The Cys128 mutant core showed a dominant-negative effect in terms of HCV-like particle production. These results suggest that this disulfide bond is critical for the HCV virion. We also obtained the results that the dbc-complex in the nucleocapsid-like structure was sensitive against proteinase K but not trypsin digestion, suggesting that the capsid is built up of a tightly packed structure of the core with its amino (N)-terminal arginine-rich region concealed inside.

## INTRODUCTION

Hepatitis C virus (HCV) infection is a major cause of chronic hepatitis, liver cirrhosis, and hepatocellular carcinoma, affecting approximately 200 million people worldwide (13, 29, 44). Current treatment strategies, including interferon coupled with ribavirin, are not effective for all patients infected with HCV. An error-prone replication strategy allows HCV to undergo rapid mutational evolution in response to immune pressure, and thus evade adaptive immune responses (10). New approaches to HCV therapy include the development of specifically targeted antiviral therapies for hepatitis C (STAT-Cs), which target such HCV proteins as NS3/4A, serine protease, and the RNA-dependent RNA polymerase NS5B (3). Despite potent antiviral activity for some of these approaches, many resistant HCV strains have been reported after treatment with existing STAT-Cs (23, 48, 51). Therefore, identification of new targets that are common to all HCV strains and are associated with low mutation rates is an area of active research.

HCV has a 9.6-kb, plus-strand RNA genome composed of a 5'-untranslated region (UTR), an open reading frame that encodes a single polyprotein of about 3000 amino acids, and a 3'-UTR. The polyprotein is processed by host and viral proteases to produce three structural proteins (core, E1, and E2) and seven nonstructural proteins (p7,

NS2, NS3, NS4A, NS4B, NS5A, and NS5B) (14, 16, 17, 22, 49). HCV core protein is produced co-translationally via carboxyl (C)-terminal cleavage to generate an immature core protein, 191 amino acids in length, on the endoplasmic reticulum (ER) (16). This protein consists of three predicted domains: the N-terminal hydrophilic domain (D1), the C-terminal hydrophobic domain (D2), and the tail domain (33), which serves as a signal peptide for the E1 envelope protein. The D1 includes a number of positively charged amino acids responsible for viral RNA binding (amino acids 1-75) (43) and the region involved in multimerization of core via homotypic interactions (amino acids 36-91 and 82-102) (32, 40) (**Supplementary Fig. 1**). The hydrophobic D2 includes the region responsible for core association with lipid droplets (LDs) (amino acids 125-144) (7, 18, 37), which accumulate in response to core production (1, 6).

Many functions of core protein have been reported (13, 38, 50). Yet because infectious HCV particles cannot be appropriately produced in currently available experimental systems, HCV particle assembly has not been elucidated to date. A cell culture system that reproduces the complete lifecycle of HCV *in vitro* was developed by Wakita et al. using a cloned HCV genome (JFH1) (53). Using this system, the assembly of infectious HCV particles was found to occur near LDs and ER-derived LD-associated membranes (36, 47). Neither the structures nor functions of the virus proteins involved

74 in virus particle assembly are known, however. To elucidate this point, we have
75 analyzed the biochemical characteristics of the proteins within the fraction containing
76 the HCV particle, and found a disulfide-bonded core protein complex. We revealed that
77 the disulfide-bonded dimer of core (dbd-core) was formed by a single cysteine residue
78 at amino-acid position 128 on the ER. The roles of the disulfide bond of the core in the
79 virus-like particle formation are discussed in this paper.

## MATERIALS AND METHODS

**Cell culture:** The HuH-7 and HuH-7.5 human hepatoma cell lines were grown in Dulbecco's modified Eagle's medium (Nacalai Tesque, Kyoto, Japan) supplemented with 10% fetal bovine serum, 100 U/ml nonessential amino acids (Invitrogen, Carlsbad, CA), and 100 μg/ml each penicillin and streptomycin sulfate (Invitrogen).

**Antibodies:** The antibodies used for immunoblotting and indirect immunofluorescence analysis were specific for core (#32-1), FLAG M2 (Sigma-Aldrich, St Louis, MO), c-myc (Sigma-Aldrich), NS5A (CL1), ADRP (StressGen, Victoria, Canada), Calnexin-NT (StressGen), and GAPDH (Chemicon, Temecula, CA). Antibodies specific for core (#32-1) were a gift from Dr Kohara (The Tokyo Metropolitan Institute of Medical Science, Japan). Rabbit polyclonal anti-NS5A CL1 antibodies have been described previously (36).

**Plasmid construction:** All plasmids were generated by inserting PCR-amplified fragments into expression plasmids. The plasmids, primer sequences, templates for the PCRs, and restriction enzyme sites used to construct the plasmids are listed in **Supplementary Table**. Plasmids pJFH1$^{E2FL}$ (full-length HCV genome with FLAG

epitope in E2 HVR), pJFH1$^{AAA99}$ (encoding a NS5A mutant of JFH1$^{E2FL}$, resulting in non-infectious HCV particles), pJFH1$^{PP/AA}$ (encoding a core mutant of JFH1$^{E2FL}$, which allows replication in cells but prevents HCV particle production), and pcDNA3-core$^{WT}$ (expression plasmid encoding full-length JFH1 core) have been previously described (36). Plasmid pJ6/JFH1, which contains the full-length HCV genome encoding structural proteins from the J6 strain and nonstructural proteins from the JFH1 strain, was kindly provided by Charles M. Rice (The Rockefeller University, New York, USA).

***In vitro* transcription:** RNA for transfection was synthesized as described previously (36). In brief, plasmids carrying the HCV RNA sequence were linearized with *Xba*I and used as templates for *in vitro* transcription with MEGAscript T7 (Ambion, Austin, TX).

**Transfection:** Ten micrograms of JFH1$^{E2FL}$, JFH1$^{C128A}$, JFH1$^{C184A}$, JFH1$^{C128/184A}$, or JFH$^{AAA99}$ and J6/JFH1 or J6/JFH1$^{AAA99}$ RNA were transfected into HuH-7 and HuH-7.5 cells ($1.0 \times 10^7$ cells) by electroporation (260 V, 0.95 μF) using a GENE PULSER II system (BioRad, Hercules, CA). Core expression plasmids were transfected into HuH-7 cells using Lipofectamine LTX (Invitrogen) according to the manufacturer's protocol.

**HCV particle precipitation:** Culture medium from HCV RNA–transfected cells were concentrated using Amicon Ultra-15 centrifugal filters with Ultracell-100 membranes (Millipore, Billerica, MA) and mixed with sucrose solution in PBS to a final sucrose concentration of 2%. This mixture was ultracentrifuged (100,000 × *g*; 4°C for 2 h) and the HCV particles were obtained as a pellet. The pellet was then suspended in culture medium for infection experiments or PBS for immunoblot analysis.

**Indirect immunofluorescence analysis:** Indirect immunofluorescence analyses of HCV infection and the cellular localization of HCV proteins were performed as described previously (36).

**Protease protection assay:** Concentrated culture medium from JFH1$^{E2FL}$ RNA–transfected HuH-7 cells was fractionated using 20~50% sucrose density gradients and the HCV RNA titer was measured in quantitative RT-PCRs as described below. Fractions with high HCV RNA titers were collected and JFH1$^{E2FL}$ particles were obtained as a pellet after ultracentrifugation (100,000 × g; 4°C for 2 h). The pellet was suspended in PBS and treated with 10 μg/ml trypsin or 5 μg/ml proteinase K in the presence or absence of 1% NP-40 at 37°C for 15 min, respectively, unless otherwise

indicated. The reaction was quenched by the addition of protease inhibitor cocktail (Nacalai Tesque) followed by SDS-PAGE under non-reducing conditions and immunoblotting specific for core protein.

**Immunoblot analysis:** Samples were subjected to SDS-PAGE in sample buffer (62.5 mM Tris-HCl [pH 7.8], 1% SDS, and 10% glycerol) with or without 5% β-ME or 50 mM DTT for reducing or non-reducing conditions, respectively. N-ethylmaleimide (NEM) (Nacalai Tesque) was added to the sample buffer to final concentration of 5 mM in indicated samples. Proteins were transferred to polyvinylidene difluoride membrane, and blocked in blocking buffer for 1 h at room temperature with gentle agitation. After incubation with primary antibodies overnight at 4°C, the membrane was washed three times for 5 min in washing buffer at RT with gentle agitation. Then, the membrane was incubated with HRP-conjugated secondary antibodies for 1 h at RT. After three washes in washing buffer, proteins were detected using Western Lightning (PerkinElmer, Waltham, MA) or ECL Advance (GE Healthcare, Buckinghamshire, England) and Kodak MXJB plus medical X-ray film (Kodak, Rochester, NY) or an LAS-4000 system (Fujifilm, Tokyo, Japan)

**Preparation of LDs:** LDs were prepared as described previously (36).

**Preparation of MMFs:** MMFs were collected as previously described (15) with some modifications. In brief, cells were collected in homogenization buffer (20 mM Tris-HCl [pH 7.8], 250 mM sucrose, and 0.1% ethanol supplemented with protease inhibitor cocktail) and homogenized on ice using 40 strokes of a dounce homogenizer. The samples were then centrifuged at 1000 × *g* for 10 min at 4°C. Supernatant was collected in a new tube and centrifuged again at 16,000 × *g* for 20 min at 4°C. Supernatant was further centrifuged at 100,000 × *g* for 60 min at 4°C. The MMF precipitate was homogenized in lysis buffer (1% NP-40, 0.1% SDS, 20 mM Tris-HCl [pH 8.0], 150 mM NaCl, 1 mM EDTA, and 10% glycerol supplemented with protease inhibitor cocktail) using a dounce homogenizer.

**Quantitative reverse transcription (qRT)-PCR analysis:** qRT-PCR analysis for the HCV RNA titer was performed as described previously (36).

**Enzyme-linked immunosorbent assay (ELISA) specific for core:** Core in culture medium was quantified using an ELISA according to the manufacturer's protocol (HCV

antigen ELISA test; Ortho-Clinical Diagnostics, Raritan, NJ).

**RNA-protein binding precipitation assay:** Core$^{WT}$ or core$^{C128A}$ were translated *in vitro* from pcDNA3-core$^{WT}$ or pcDNA3-core$^{C128A}$, respectively, using the TNT Coupled Rabbit Reticulocyte Lysate system (Promega, Madison, WI) according to the manufacturer's protocol. These proteins were incubated with poly-U agarose (Sigma) in 50 mM HEPES (pH 7.4), 100 mM NaCl, 0.1% NP-40, and 20 U RNase inhibitor at 4°C for 2 h with or without RNase A. After five washes, resin-bound core proteins were immunoblotted.

## RESULTS

### The HCV particle contains core complex formed by a disulfide bond

To analyze the core protein of the HCV particle, we first subjected the concentrated culture medium of HuH-7 cells transfected with *in vitro* transcribed JFH1$^{E2FL}$ RNA to ultracentrifugation. After the resulting pellet was resuspended in culture medium, we confirmed the presence of infectious HCV particles based on infectivity against HuH-7.5 cells (**Fig. 1a**). The infectious JFH1$^{E2FL}$ particle–containing pellet was separated by SDS-PAGE under non-reducing conditions, and immunoblot analysis showed the presence of a core antibody–reactive protein that was approximately twice the size of core (38 kDa), in addition to the expected 19-kDa core protein (**Fig. 1b**, lane 1). Because treatment with dithiothreitol (DTT) eliminated the larger core antibody–reactive band while levels of core monomer increased (**Fig. 1b**, lanes 2-6), the larger protein likely represented a core-containing complex formed by disulfide bonds. This complex was also found in J6/JFH1-derived particles (**Supplementary Fig. 2**), indicating that the complex was not specific for JFH1$^{E2FL}$.

To determine whether the core complex is a component of the HCV particle, a protease protection assay was performed using RNase-resistant HCV particles fractionated based on buoyant density. Concentrated culture medium from HuH-7 cells

197 transfected with *in vitro* transcribed JFH1$^{E2FL}$ RNA were fractionated using a 20-50%
198 sucrose density gradient and JFH1$^{E2FL}$ particles which were presumed to contain both
199 infectious and non-infectious particles, were collected from fractions with high HCV
200 RNA titers using ultracentrifugation (**Fig. 2a**, fraction #8 to #13). The core protein from
201 the collected fractions was analyzed by immunoblotting after SDS-PAGE under the
202 non-reducing condition, showing only the core complex (**Fig. 1c**, right panel).

203 To examine whether the complex contributes to the infectivity of the particles,
204 we analyzed the core complex in the fractions containing infectious and non-infectious
205 HCV particles (fraction #9 and #11 of **Fig. 2a**, filled and open arrowheads, respectively).
206 Both infectious and non-infectious HCV particle containing fraction consists the core
207 complex (**Fig. 2b**). To confirm this further, a pellet containing mutant JFH1$^{AAA99}$
208 particles—a mutant of JFH1$^{E2FL}$ that produces primarily non-infectious particles
209 (36)—was analyzed in a similar manner. These core complexes were found in both
210 pelleted particles of JFH1$^{AAA99}$ and J6/JFH1$^{AAA99}$ which was a mutant J6/JFH1 with
211 similar substitution to JFH1$^{AAA99}$ (**Supplementary Fig. 2**). These results indicated that
212 the core complex was present in both the infectious and non-infectious HCV-like
213 particles.

214 The core monomer observed in the pellet samples (**Fig. 1b**) may be from the

secreted core or the debris of apoptotic cells, because the core is known to be secreted from cells expressing this protein under particular conditions (42), and JFH1 strain is known to cause apoptosis (45). The core complex–specific signals in the HCV particles seem to be increased with the NP-40 treated samples for some unknown reason (**Fig. 1c**; lanes 1 and 2). Although the intermolecular disulfide bond is known to be artificially formed in denaturing SDS-PAGE in the absence of reducing agents, the core complex was still observed even in the presence of NEM, which is alkylating agent for free sulfhydryls, during sample preparation (**Fig. 2c**), indicating that the core complex was naturally present in the virus-like particles.

The HCV nucleocapsid is covered with lipid membranes and E1 and E2 envelope proteins, making it resistant to proteases. As expected, in the absence of NP-40, the core complex was resistant to proteinase K (**Fig. 1c**, lane 3), whereas proteinase K was able to digest core protein in whole-cell lysates collected from $JFH1^{E2FL}$-transfected HuH-7 cells (**Fig. 1c**, left panel). Disrupting the envelope structure with NP-40 made the core complex susceptible to proteinase K treatment (**Fig. 1c**, lane 4), indicating that the core complex was indeed a component of the HCV particle.

**The disulfide-bonded core complex (dbc-complex) forms on the ER**

233 To investigate the subcellular site at which the dbc-complex forms, LD and
234 microsomal membrane fractions (MMFs) from JFH1$^{E2FL}$ replicating HuH-7 cells were
235 analyzed by immunoblotting. We first analyzed the dbc-complex in LDs, because the
236 LD is involved in infectious HCV particle formation (36, 47). The purity of the LD
237 fraction was determined using immunoblot analysis of calnexin and adipocyte
238 differentiation-related protein (ADRP), an ER and an LD marker protein, respectively
239 (**Fig. 3a**, upper panel). The core protein was then analyzed in the LD fraction. As shown
240 in **Figure 3a** (lower panel), the dbc-complex was observed in the LD fraction from
241 JFH1$^{E2FL}$ RNA–transfected HuH-7 cells. We next analyzed the core protein in the
242 ER-containing MMF, because the core protein is first translated and processed on the
243 ER (16). As shown in **Figure 3b**, the dbc-complex was observed in the MMF from
244 JFH1$^{E2FL}$ RNA–transfected HuH-7 cells. These results suggest that the dbc-complex is
245 first formed at the ER. To assess the possibility that dbc-complex-containing HCV
246 particles were also assembled on the ER, the sensitivity of the dbc-complex to protease
247 treatment was analyzed. The dbc-complex in the MMF was susceptible to protease
248 treatment in the absence of NP-40, indicating that the dbc-complex on the ER was not
249 part of a HCV particle (data not shown).
250

**dbc-Complex is most likely a disulfide-bonded dimer form of the core**

In order to examine whether the core itself have a potential to form dbc-complex, we analyzed dbc-complex formation of full length wild-type core ($core^{WT}$) expressed from pcDNA3-$core^{WT}$ (36), the expression plasmid encoding 191 amino acid full length core of JFH1 strain. We used this expression plasmid because the core from this plasmid was likely to be processed correctly enough to produce infectious HCV particles when co-transfected with $JFH1^{dc3}$ RNA, which is a core deletion mutant of JFH1 (36). As results, the dbc-complex formation was observed from the MMF of $core^{WT}$ expressing cells both in the absence and the presence of NEM (**Fig. 4b**; lane 2 and data not shown, respectively). We next investigated the effect of the amino acid region of E1 on the production of dbc-complex, because it has been reported that the efficient processing of core protein is dependent on the presence of some E1 sequence to ensure the insertion of the signal sequence for E1 in the translocon/membrane machinery (34). Then the dbc-complex was also observed when the core was expressed from a pcDNA3-C-E1/25, which encodes the full length core followed by the N-terminal 25 amino acid sequence of E1 to ensure that the core is processed properly (**Supplementary Fig. 3a**). These data showed that the dbc-complex was formed by expression of the core protein only in the cells.

Next, we examined the structural components of the dbc-complex. Because the dbc-complex was twice the size of a core monomer, it likely was disulfide-bonded dimer form of the core (dbd-core). So, we investigated whether the core molecules with different tags were able to form the dbd-core. We first generated expression plasmids encoding core with the N-terminal FLAG and Myc tags (pcDNA3-FLAG-core and pcDNA3-Myc-core, respectively; **Fig. 4a**). The tagged core proteins were expressed or co-expressed with core$^{WT}$ in HuH-7 cells and the MMF was analyzed by SDS-PAGE. The FLAG or Myc tag shifted the positions of the monomer and the complex bands (**Fig. 4b**; lanes 3 and 4), compared with the core$^{WT}$ (**Fig. 4b**; lane 2). When the core$^{WT}$ was co-expressed with FLAG-core or Myc-core, the core complex with an intermediately size was observed in addition to the bands obtained when the constructs were independently expressed (**Fig. 4b**; lanes 5 and 6, filled arrows); the intermediate band disappeared after treatment with β-mercaptoethanol (β-ME) (**Supplementary Fig. 3b**; lanes 11 and 12, filled arrows), indicating that core$^{WT}$ and tagged core formed a heteromeric disulfide-bonded dimer. These results demonstrated that the dbc-complex on the ER is a dbd-core. Although we tried to detect the hetero-/homo-dimer consisting the tagged-core by using anti-FLAG or anti-Myc antibodies, these dimers but the monomeric forms of the tagged-core were not detected, possibly because of the less

sensitivity and specificity of the antibodies compared to the anti-core antibody we used especially against epitopes in the dbd-core. Above results coupled with the similarity of the molecular size and sensitivity against β-ME and DTT, suggested the dbc-complex in the HCV particle is most likely a dbd-core.

**Core cysteine residue 128 (Cys128) mediates dbd-core formation**

Our results showed that core from JFH1$^{E2FL}$ forms a disulfide-bonded dimer on the ER. A search for cysteine residues in JFH1$^{E2FL}$ core identified amino-acid positions 128 (Cys128) and 184 (Cys184) (**Supplementary Fig. 1**). These residues are highly conserved in core proteins from the approximately 2000 reported HCV strains (HCVdb, http://www.hcvdb.org/; Hepatitis Virus Database; http://s2as02.genes.nig.ac.jp/). To determine which cysteine residue meditated disulfide bond formation, we generated point mutations in JFH1$^{E2FL}$ that substituted Cys128 and/or Cys184 with Alanine (Ala) (C128A, C184A and C128/184A in JFH1$^{C128A}$, JFH1$^{C184}$ and JFH1$^{C128/184A}$, respectively; **Fig. 5a**). As shown in **Figure 5b**, core protein from JFH1$^{C128A}$ and JFH1$^{C128/184A}$ failed to form a dbd-core under non-reducing condition, whereas core protein from JFH1$^{C184A}$ formed the dimer, indicating that Cys128 was the responsible residue. Similar results were observed when Cys was substituted to Serine (Ser) instead of Ala

(**Supplementary Fig. 5c**). Recently, Majeau et al. reported that the core protein of J6/JFH1 strain with Cys128 substitutions to Ala or Ser were instable in both *Pichia pastoris* and human hepatoma cell line HuH-7.5 (31), although we did not detect any noticeable degradation of the mutant cores of JFH1 strain (**Fig. 5b** and **Supplementary Fig. 5c**). This difference may resulted from difference in sample preparation as we used full length genome of $JFH1^{E2FL}$ strain, bearing JFH1 strain core, and HuH-7 cells instead of core expressing plasmid for J6 strain and HuH-7.5.

To exclude the possibility that mutation of Cys128 inhibited dbd-core formation by creating a conformational change, T127A and G129A core mutants ($JFH1^{T127A}$ and $JHF1^{G129A}$, respectively) were created and examined for the effects on dbd-core formation and infectious virus particle production. These mutants formed dbd-core and infectious HCV particles were detected in the culture medium (**Supplementary Fig. 4a-c**), supporting an essential role for Cys128 in dbd-core and particle formation.

**dbd-Core contributes to HCV particle production**

To examine the functional roles of dbd-core, infectious HCV particle production, HCV replication efficiency, co-localization of core and the LD, and

RNA-binding of mutant and wild-type ($JFH1^{E2FL}$) core were evaluated. Culture medium from HuH-7 cells transfected with $JFH1^{C128A}$ or $JFH1^{C128/184A}$ RNA contained significantly fewer infectious HCV particles compared with results obtained with $JFH1^{E2FL}$ or $JFH1^{C184A}$ RNA (**Fig. 5c**). We also found significant decreases in the levels of HCV RNA and the core protein in the culture medium of HuH-7 cells transfected with $JFH1^{C128A}$ or $JFH1^{C128/184A}$ RNA (**Fig. 5d, e**). Similar results were observed with J6/JFH1 C128A or C128/184A mutant strain (data not shown). To investigate whether these results were due to suppressed HCV replication, HCV RNA and protein levels in cells transfected with mutant RNA were analyzed using qRT-PCR and immunoblot analyses, respectively. Compared with results obtained with $JFH1^{E2FL}$, no significant changes were observed in the cellular HCV RNA titer at days 1, 3 and 5 post-transfection or in the expression of the HCV nonstructural protein NS5A (**Fig. 6a, b**). This indicated that substitution of Cys128 did not significantly affect HCV RNA genome replication or viral protein production, demonstrating that the dbd-core functions during HCV particle production rather than HCV genome replication. Similar results were observed using RNA of JFH1 mutant strain which Cysteine of position 128 were substituted to Ser instead of Ala; $JFH1^{C128S}$ (**Supplementary Fig. 5a, b, d**).

The subcellular localizations of core and NS5A in HuH-7 cells transfected with

HCV RNA were investigated using indirect immunofluorescence and confocal microscopy, because recruiting HCV proteins to the LD is an important step in infectious HCV particle production (36, 47) and core trafficking to the LD is dependent on SPP-mediated cleavage of the tail region (34, 41). JFH1$^{C128A}$ mutant core and NS5A were efficiently trafficked to the LD, as was observed with wild-type JHF1$^{E2FL}$ (**Fig. 6c**), suggesting that SPP cleavage and core maturation were not affected by the C128A mutation. Similar results were obtained with core derived from JFH1$^{C184A}$ and JFH1$^{C128/184A}$ (**Supplementary Fig. 6**), and also, Ser mutant JFH1$^{C128S}$ (**Supplementary Fig. 5e**).

Because HCV core protein can bind RNA, including the HCV genome during viral particle assembly (43), we analyzed RNA binding by core using *in vitro* translated core$^{C128A}$, core$^{WT}$, and poly-uridine (U) agarose resin. Core$^{C128A}$ and core$^{WT}$ similarly bound with poly-U resin (**Fig. 6d**).

**dbd-Core is important for HCV particle assembly**

The mutational analysis of core indicated that core$^{C128A}$ and core$^{WT}$ similarly localize to LDs, recruit NS proteins to the LD, and bind to RNA. Moreover, this mutation did not markedly affect HCV genome replication. How does core$^{C128A}$ affect

359 the production of HCV particles? An important function of core protein is
360 multimerization, which is followed by capsid construction and packaging of the RNA
361 genome in the viral particles. We therefore determined whether core$^{C128A}$ had a
362 dominant-negative effect on virus-like particle production. Wild-type JFH1$^{E2FL}$ RNA
363 and different amounts of JFH1$^{C128A}$ RNA were co-transfected into HuH-7 cells and the
364 HCV RNA titer and infectivity of the virus-like particles in the culture medium were
365 analyzed. As expected, the HCV RNA titer in the cells increased with higher levels of
366 transfected RNA (**Supplementary Fig. 7a**). In contrast, the HCV RNA titer and
367 infectivity in the culture medium decreased in a JFH1$^{C128A}$ RNA dose–dependent
368 manner when this mutant RNA was co-transfected with wild-type RNA (**Fig. 7a, b**).
369 This suppressive effect was not observed when either wild-type RNA or core deletion
370 mutant JFH1$^{dc3}$ RNA was used instead of mutant RNA in a similar experiment
371 (**Supplementary Fig. 7b-e**), indicating that higher levels of HCV RNA alone did not
372 inhibit HCV particle production. Thus, core$^{C128A}$ had a dominant-negative effect on
373 HCV particle production. Together, these results suggest that dbd-core is involved in the
374 assembly of HCV particles.
375
376 **The nucleocapsid-like particle of HCV was resistant to trypsin treatment**

377 To further investigate the structure of the HCV nucleocapsid-like particle most
378 likely formed by dbd-core, we examined the sensitivity of the particle to trypsin, which
379 cleaves polypeptides at the C-terminal end of basic residues. Whereas trypsin digested
380 core in the whole-cell lysates (**Fig. 8a**, left panel), dbd-core from buoyant
381 density–fractionated JFH1$^{E2FL}$ particles was resistant to digestion despite NP-40
382 treatment (**Fig. 8a**, right panel), although it was sensitive to proteinase K which have a
383 broad specificity (**Fig. 1c**). The N-terminal hydrophilic domain of the core protein
384 (from residues 6-121) contains a number of trypsin cleavage sites (25 sites, in JHF1
385 strain) (**Supplementary Fig. 1**), suggesting that the N-terminal domain faces inward
386 and/or the conformation prevents protease access. To address this idea, buoyant
387 density–fractionated JFH1$^{E2FL}$ particles were treated with trypsin under more strict
388 conditions in the presence of NP-40. Cleavage of dbd-core by various levels of trypsin
389 correlated with the appearance of a shorter molecule (**Fig. 8b,** white arrowhead). The
390 shorter molecule was presumed to be partially digested dbd-core with an intact
391 N-terminal region because it was recognized by anti-core antibodies, which bind an
392 epitope located in amino-acids 20-40 of core (personal communication from Dr. M.
393 Kohara, The Tokyo Metropolitan Institute of Medical Science, Japan). These results
394 suggest that dbd-core is assembled into the nucleocapsid-like particle such that most of

the N-terminal domain is inside.

## DISCUSSION

In this study, we have shown that the nucleocapsid-like particle of HCV contains most likely a dimer of core protein that is stabilized by a disulfide bond. Mutational analysis revealed that Cys128 forms the disulfide bond between core monomers. Several reports have shown that disulfide bonds in the capsid proteins of some viruses are involved in virus particle assembly and stabilization of the viral capsid structure (4, 21, 27, 28, 57); these viruses are characterized by icosahedral nucleocapsids. Because, like these viruses, the HCV virion is spherical (2, 20), it has been suggested that HCV may contain a nucleocapsid with a similar structure (20). We found the dbc-complex which is most likely to be the dbd-core in $JFH1^{E2FL}$ virus-like particles (**Figs. 1c and 8a**). The dbd-core in the capsid structure was digested by proteinase K but not trypsin in the presence of NP-40 (**Figs. 1c and 8a, lane 4**). The resistance to trypsin suggested a tight conformation for dbd-core in the capsid with no exposed trypsin cleavage sites. The truncated form of dbd-core that was observed under certain trypsin treatment conditions likely resulted from cleavage in the C-terminal portion of the protein (e.g., arginine residues at positions 149 and 156) (**Supplementary Fig. 1**), although it is possible that the truncation of dbd-core was due to non-specific cleavage by trypsin. These results imply that dbd-core is configured such that the N-

414 and C-terminal ends are located at the inner and outer surface of the capsid, respectively.
415 Because the N-terminal region of core includes the RNA binding domain (43), the HCV
416 RNA genome likely interacts with core as it is packed in the nucleocapsid. On the other
417 hand, the C-terminal hydrophobic domain probably faces the lipid membranes to form
418 the envelope structure. Only part of the N-terminal hydrophilic region of the core
419 protein has been structurally examined using X-ray crystal structural analysis (35), and
420 using structural bioinformatics and nuclear magnetic resonance analysis (11). Although
421 the C-terminal half of core has been structurally investigated by bioinformatics (8), the
422 3D structure containing the Cys128 residue is unknown. Thus, determination of the
423 structure of the core in the nucleocapsid containing Cys128 residue should be required
424 for understanding the whole structure of this protein in the virus particles.

425 Because co-transfection of JFH1$^{C128A}$ RNA with wild-type JFH1$^{E2FL}$ RNA
426 inhibited particle production in a mutant RNA dose-dependent manner (**Fig. 7a, b**), the
427 C128A core variant clearly inhibited HCV particle formation by wild-type core. Cys128
428 was also reported previously to be a residue included in the region important for the
429 production of infectious HCV (39). This residue is located near the N-terminal end of
430 the hydrophobic region of the core (amino acids 122-177) and belongs to the
431 hydrophilic side of an amphipathic helix expected to interact in-plane of the membrane

interface (7). Therefore, it is possible to think that the dbd-core formation via Cys128 can stabilize the interaction between core and the membranes. The N-terminal half of core (amino acids 1-124) reportedly assembles into nucleocapsid-like particles in the presence of 5'-UTR from HCV RNA (24), suggesting that some nucleocapsid-like particles may assemble via only homotypic interactions from the core protein. In addition to weak homotypic interactions, the HCV core protein forms a disulfide bond to stabilize the capsid structure, thus making dbd-core indispensable in the stable virus-like particle. We observed that culture medium from JFH1$^{C128A}$ or JFH1$^{C128S}$-transfected cells included slight infectivity (**Fig. 5c** or **Supplementary Fig. 5d**). This made us speculate that this mutant may produce some infective particle-like structure formed by homotypic interaction of the core. Such a slight infectivity may have reflected the optimized *in vitro* culture conditions compared with *in vivo* conditions, allowing relatively unstable virus particles to survive.

A nucleocapsid must be resistant to environmental degradation, yet still be able to disassemble after infection. Disulfide bonds could help with these process by switching between a stable and unstable virus capsid based on different intracellular and extracellular oxidation conditions (12, 30). During the virus life cycle, the disulfide bond strengthens the viral capsid structure and protects the viral genome from oxidative

conditions and cellular nucleases when virus particles are formed. Upon infection, the disulfide bond may be cleaved under cytoplasmic reducing conditions, thereby releasing the viral genome into the cell for replication. HCV may utilize the core protein disulfide bond in this way as HCV enters the host cell via clathrin-mediated endocytosis (5) into a low-pH, endosomal compartment (25, 52); this is presumably followed by endosomal membrane fusion and release of the viral capsid into the cytoplasm (38).

Treatment of HCV with pegylated interferon in combination with ribavirin is not effective for all patients. Recently, drugs targeting the viral proteins NS3/4A and NS5B have been examined in clinical trials. Although these drugs are relatively specific, resulting in fewer side effects and potent antiviral activity, monotherapy can be complicated by rapidly emerging resistant variants, carrying mutations that reduce drug efficacy, perhaps due to conformational changes in the target (23, 48, 51). Therefore, viral proteins that are highly conserved among strains and those characterized by low mutation rates may be better targets for drug development. Because the core protein is the most conserved HCV protein and Cys128 is conserved among almost all examined HCV strains, drugs that interact with Cys128 and/or region around or near this residue will likely show broad spectrum efficacy to block the stable infectious particle formation. Structural analysis of dbd-core should aid the development of new STAT-Cs

that target Cys128 by direct interaction with the sulfide group and/or region around this residue. Until now and still, the mechanism of disulfide bond formation of core on the ER is unknown. Dimerization of capsid protein by disulfide bond has been reported in some enveloped viruses (9, 19, 54, 56), although some were shown not to be important for virus particle formation (26, 55). Unlike the vaccinia virus (46), no redox system of its own has been reported for these viruses. Therefore, further investigations addressing the mechanisms underlying dbd-core formation on the ER may reveal new mechanism for disulfide bond formation of viral proteins in infected cells.

476 **ACKNOWLEDGMENTS**

477 This work was supported by grants-in-aid from the Ministry of Health, Labour and

478 Welfare of Japan and by grants-in-aid from the Japan Health Sciences Foundation.

## REFERENCES


1. **Abid, K., V. Pazienza, A. de Gottardi, L. Rubbia-Brandt, B. Conne, P. Pugnale, C. Rossi, A. Mangia, and F. Negro.** 2005. An in vitro model of hepatitis C virus genotype 3a-associated triglycerides accumulation. J Hepatol **42:**744-51.
2. **Aly, H. H., Y. Qi, K. Atsuzawa, N. Usuda, Y. Takada, M. Mizokami, K. Shimotohno, and M. Hijikata.** 2009. Strain-dependent viral dynamics and virus-cell interactions in a novel in vitro system supporting the life cycle of blood-borne hepatitis C virus. Hepatology **50:**689-96.
3. **Asselah, T., Y. Benhamou, and P. Marcellin.** 2009. Protease and polymerase inhibitors for the treatment of hepatitis C. Liver Int **29 Suppl 1:**57-67.
4. **Baron, M. D., and K. Forsell.** 1991. Oligomerization of the structural proteins of rubella virus. Virology **185:**811-9.
5. **Blanchard, E., S. Belouzard, L. Goueslain, T. Wakita, J. Dubuisson, C. Wychowski, and Y. Rouille.** 2006. Hepatitis C virus entry depends on clathrin-mediated endocytosis. J Virol **80:**6964-72.
6. **Boulant, S., M. W. Douglas, L. Moody, A. Budkowska, P. Targett-Adams, and J. McLauchlan.** 2008. Hepatitis C virus core protein induces lipid droplet redistribution in a microtubule- and dynein-dependent manner. Traffic **9:**1268-82.
7. **Boulant, S., R. Montserret, R. G. Hope, M. Ratinier, P. Targett-Adams, J. P. Lavergne, F. Penin, and J. McLauchlan.** 2006. Structural determinants that target the hepatitis C virus core protein to lipid droplets. J Biol Chem **281:**22236-47.
8. **Boulant, S., C. Vanbelle, C. Ebel, F. Penin, and J. P. Lavergne.** 2005. Hepatitis C virus core protein is a dimeric alpha-helical protein exhibiting membrane protein features. J Virol **79:**11353-65.
9. **Cornillez-Ty, C. T., and D. W. Lazinski.** 2003. Determination of the multimerization state of the hepatitis delta virus antigens in vivo. J Virol **77:**10314-26.
10. **Dustin, L. B., and C. M. Rice.** 2007. Flying under the radar: the immunobiology of hepatitis C. Annu Rev Immunol **25:**71-99.
11. **Duvignaud, J. B., C. Savard, R. Fromentin, N. Majeau, D. Leclerc, and S. M. Gagne.** 2009. Structure and dynamics of the N-terminal half of hepatitis C virus core protein: an intrinsically unstructured protein. Biochem Biophys Res Commun **378:**27-31.
12. **Freedman, R. B., B. E. Brockway, and N. Lambert.** 1984. Protein disulphide-isomerase and the formation of native disulphide bonds. Biochem Soc Trans **12:**929-32.
13. **Giannini, C., and C. Brechot.** 2003. Hepatitis C virus biology. Cell Death Differ **10 Suppl 1:**S27-38.
14. **Grakoui, A., C. Wychowski, C. Lin, S. M. Feinstone, and C. M. Rice.** 1993. Expression and

identification of hepatitis C virus polyprotein cleavage products. J Virol **67:**1385-95.

15. **Higashi, Y., H. Itabe, H. Fukase, M. Mori, Y. Fujimoto, R. Sato, T. Imanaka, and T. Takano.** 2002. Distribution of microsomal triglyceride transfer protein within sub-endoplasmic reticulum regions in human hepatoma cells. Biochim Biophys Acta **1581:**127-36.

16. **Hijikata, M., N. Kato, Y. Ootsuyama, M. Nakagawa, and K. Shimotohno.** 1991. Gene mapping of the putative structural region of the hepatitis C virus genome by in vitro processing analysis. Proc Natl Acad Sci U S A **88:**5547-51.

17. **Hijikata, M., H. Mizushima, Y. Tanji, Y. Komoda, Y. Hirowatari, T. Akagi, N. Kato, K. Kimura, and K. Shimotohno.** 1993. Proteolytic processing and membrane association of putative nonstructural proteins of hepatitis C virus. Proc Natl Acad Sci U S A **90:**10773-7.

18. **Hope, R. G., and J. McLauchlan.** 2000. Sequence motifs required for lipid droplet association and protein stability are unique to the hepatitis C virus core protein. J Gen Virol **81:**1913-25.

19. **Hu, H. M., K. N. Shih, and S. J. Lo.** 1996. Disulfide bond formation of the in vitro-translated large antigen of hepatitis D virus. J Virol Methods **60:**39-46.

20. **Ishida, S., M. Kaito, M. Kohara, K. Tsukiyama-Kohora, N. Fujita, J. Ikoma, Y. Adachi, and S. Watanabe.** 2001. Hepatitis C virus core particle detected by immunoelectron microscopy and optical rotation technique. Hepatol Res **20:**335-347.

21. **Jeng, K. S., C. P. Hu, and C. M. Chang.** 1991. Differential formation of disulfide linkages in the core antigen of extracellular and intracellular hepatitis B virus core particles. J Virol **65:**3924-7.

22. **Kato, N., M. Hijikata, Y. Ootsuyama, M. Nakagawa, S. Ohkoshi, T. Sugimura, and K. Shimotohno.** 1990. Molecular cloning of the human hepatitis C virus genome from Japanese patients with non-A, non-B hepatitis. Proc Natl Acad Sci U S A **87:**9524-8.

23. **Kieffer, T. L., A. D. Kwong, and G. R. Picchio.** 2009. Viral resistance to specifically targeted antiviral therapies for hepatitis C (STAT-Cs). J Antimicrob Chemother.

24. **Kim, M., Y. Ha, and H. J. Park.** 2006. Structural requirements for assembly and homotypic interactions of the hepatitis C virus core protein. Virus Res **122:**137-43.

25. **Koutsoudakis, G., A. Kaul, E. Steinmann, S. Kallis, V. Lohmann, T. Pietschmann, and R. Bartenschlager.** 2006. Characterization of the early steps of hepatitis C virus infection by using luciferase reporter viruses. J Virol **80:**5308-20.

26. **Lee, J. Y., D. Hwang, and S. Gillam.** 1996. Dimerization of rubella virus capsid protein is not required for virus particle formation. Virology **216:**223-7.

27. **Li, M., P. Beard, P. A. Estes, M. K. Lyon, and R. L. Garcea.** 1998. Intercapsomeric disulfide bonds in papillomavirus assembly and disassembly. J Virol **72:**2160-7.

28. **Li, P. P., A. Nakanishi, S. W. Clark, and H. Kasamatsu.** 2002. Formation of transitory intrachain and interchain disulfide bonds accompanies the folding and oligomerization of simian

virus 40 Vp1 in the cytoplasm. Proc Natl Acad Sci U S A **99:**1353-8.

29. **Liang, T. J., L. J. Jeffers, K. R. Reddy, M. De Medina, I. T. Parker, H. Cheinquer, V. Idrovo, A. Rabassa, and E. R. Schiff.** 1993. Viral pathogenesis of hepatocellular carcinoma in the United States. Hepatology **18:**1326-33.

30. **Liljas, L.** 1999. Virus assembly. Curr Opin Struct Biol **9:**129-34.

31. **Majeau, N., R. Fromentin, C. Savard, M. Duval, M. J. Tremblay, and D. Leclerc.** 2009. Palmitoylation of hepatitis C virus core protein is important for virion production. J Biol Chem **284:**33915-25.

32. **Matsumoto, M., S. B. Hwang, K. S. Jeng, N. Zhu, and M. M. Lai.** 1996. Homotypic interaction and multimerization of hepatitis C virus core protein. Virology **218:**43-51.

33. **McLauchlan, J.** 2000. Properties of the hepatitis C virus core protein: a structural protein that modulates cellular processes. J Viral Hepat **7:**2-14.

34. **McLauchlan, J., M. K. Lemberg, G. Hope, and B. Martoglio.** 2002. Intramembrane proteolysis promotes trafficking of hepatitis C virus core protein to lipid droplets. EMBO J **21:**3980-8.

35. **Menez, R., M. Bossus, B. H. Muller, G. Sibai, P. Dalbon, F. Ducancel, C. Jolivet-Reynaud, and E. A. Stura.** 2003. Crystal structure of a hydrophobic immunodominant antigenic site on hepatitis C virus core protein complexed to monoclonal antibody 19D9D6. J Immunol **170:**1917-24.

36. **Miyanari, Y., K. Atsuzawa, N. Usuda, K. Watashi, T. Hishiki, M. Zayas, R. Bartenschlager, T. Wakita, M. Hijikata, and K. Shimotohno.** 2007. The lipid droplet is an important organelle for hepatitis C virus production. Nat Cell Biol **9:**1089-97.

37. **Moradpour, D., C. Englert, T. Wakita, and J. R. Wands.** 1996. Characterization of cell lines allowing tightly regulated expression of hepatitis C virus core protein. Virology **222:**51-63.

38. **Moradpour, D., F. Penin, and C. M. Rice.** 2007. Replication of hepatitis C virus. Nat Rev Microbiol **5:**453-63.

39. **Murray, C. L., C. T. Jones, J. Tassello, and C. M. Rice.** 2007. Alanine scanning of the hepatitis C virus core protein reveals numerous residues essential for production of infectious virus. J Virol **81:**10220-31.

40. **Nolandt, O., V. Kern, H. Muller, E. Pfaff, L. Theilmann, R. Welker, and H. G. Krausslich.** 1997. Analysis of hepatitis C virus core protein interaction domains. J Gen Virol **78 ( Pt 6):**1331-40.

41. **Okamoto, K., Y. Mori, Y. Komoda, T. Okamoto, M. Okochi, M. Takeda, T. Suzuki, K. Moriishi, and Y. Matsuura.** 2008. Intramembrane processing by signal peptide peptidase regulates the membrane localization of hepatitis C virus core protein and viral propagation. J Virol **82:**8349-61.

42. **Sabile, A., G. Perlemuter, F. Bono, K. Kohara, F. Demaugre, M. Kohara, Y. Matsuura, T. Miyamura, C. Brechot, and G. Barba.** 1999. Hepatitis C virus core protein binds to apolipoprotein AII and its secretion is modulated by fibrates. Hepatology **30:**1064-76.

43. **Santolini, E., G. Migliaccio, and N. La Monica.** 1994. Biosynthesis and biochemical properties of the hepatitis C virus core protein. J Virol **68:**3631-41.

44. **Seeff, L. B., and J. H. Hoofnagle.** 2003. Appendix: The National Institutes of Health Consensus Development Conference Management of Hepatitis C 2002. Clin Liver Dis **7:**261-87.

45. **Sekine-Osajima, Y., N. Sakamoto, K. Mishima, M. Nakagawa, Y. Itsui, M. Tasaka, Y. Nishimura-Sakurai, C. H. Chen, T. Kanai, K. Tsuchiya, T. Wakita, N. Enomoto, and M. Watanabe.** 2008. Development of plaque assays for hepatitis C virus-JFH1 strain and isolation of mutants with enhanced cytopathogenicity and replication capacity. Virology **371:**71-85.

46. **Senkevich, T. G., C. L. White, E. V. Koonin, and B. Moss.** 2000. A viral member of the ERV1/ALR protein family participates in a cytoplasmic pathway of disulfide bond formation. Proc Natl Acad Sci U S A **97:**12068-73.

47. **Shavinskaya, A., S. Boulant, F. Penin, J. McLauchlan, and R. Bartenschlager.** 2007. The lipid droplet binding domain of hepatitis C virus core protein is a major determinant for efficient virus assembly. J Biol Chem **282:**37158-69.

48. **Shimakami, T., R. E. Lanford, and S. M. Lemon.** 2009. Hepatitis C: recent successes and continuing challenges in the development of improved treatment modalities. Curr Opin Pharmacol **9:**537-44.

49. **Tellinghuisen, T. L., M. J. Evans, T. von Hahn, S. You, and C. M. Rice.** 2007. Studying hepatitis C virus: making the best of a bad virus. J Virol **81:**8853-67.

50. **Tellinghuisen, T. L., and C. M. Rice.** 2002. Interaction between hepatitis C virus proteins and host cell factors. Curr Opin Microbiol **5:**419-27.

51. **Thompson, A. J., and J. G. McHutchison.** 2009. Antiviral resistance and specifically targeted therapy for HCV (STAT-C). J Viral Hepat **16:**377-87.

52. **Tscherne, D. M., C. T. Jones, M. J. Evans, B. D. Lindenbach, J. A. McKeating, and C. M. Rice.** 2006. Time- and temperature-dependent activation of hepatitis C virus for low-pH-triggered entry. J Virol **80:**1734-41.

53. **Wakita, T., T. Pietschmann, T. Kato, T. Date, M. Miyamoto, Z. Zhao, K. Murthy, A. Habermann, H. G. Krausslich, M. Mizokami, R. Bartenschlager, and T. J. Liang.** 2005. Production of infectious hepatitis C virus in tissue culture from a cloned viral genome. Nat Med **11:**791-6.

54. **Wootton, S. K., and D. Yoo.** 2003. Homo-oligomerization of the porcine reproductive and respiratory syndrome virus nucleocapsid protein and the role of disulfide linkages. J Virol **77:**4546-57.

622 55. **Zhou, S., and D. N. Standring.** 1992. Cys residues of the hepatitis B virus capsid protein are
623 not essential for the assembly of viral core particles but can influence their stability. J Virol
624 **66:**5393-8.
625 56. **Zhou, S., and D. N. Standring.** 1992. Hepatitis B virus capsid particles are assembled from
626 core-protein dimer precursors. Proc Natl Acad Sci U S A **89:**10046-50.
627 57. **Zweig, M., C. J. Heilman, Jr., and B. Hampar.** 1979. Identification of disulfide-linked protein
628 complexes in the nucleocapsids of herpes simplex virus type 2. Virology **94:**442-50.

## FIGURE LEGENDS

**Figure 1.** The HCV-like particle consists of a core complex formed by a disulfide bond. (**a**) The infectivity of the pellet fraction collected from concentrated culture medium from JFH1$^{E2FL}$ RNA–transfected HuH-7 cells was analyzed as described in the Materials and Methods. "input" represents the same volume of concentrated culture medium used to pellet the virus-like particles. (**b**) Immunoblot analysis of the core in pellets containing JFH1$^{E2FL}$ virus particles treated with various levels of DTT (lanes 1, 2, 3, 4, 5 and 6 represent 0, 1.56, 3.13, 6.25, 12.5 and 25 mM, respectively). (**c**) Immunoblot analysis of core in JFH1$^{E2FL}$ particles collected from sucrose density gradient fractions with high HCV RNA titers (particle) (**Fig. 2a,** fraction #8 to #13) and treated with 5 μg/ml proteinase K at 3°C for 15 min in the presence or absence of 1% NP-40 (right panel). As a positive control, whole-cell lysate (WCL) prepared from JFH1$^{E2FL}$ RNA–transfected HuH-7 cells in lysis buffer was treated with 5 μg/ml proteinase K at 37°C for 15 min (left panel). Data are representative of three independent experiments.

**Figure 2.** HCV nucleocapsid-like particle consists of core complex. (**a**) HCV RNA titer in culture medium separated on a 20-50% sucrose density gradient. Concentrated

culture medium from JFH1$^{E2FL}$ RNA–transfected HuH-7 cells were treated with RNase and separated on a 20-50% sucrose density gradient. Fractions were obtained from the bottom to the top of the tube (#1 to #16). The HCV RNA titer and infectivity of each fraction were analyzed by real-time qRT-PCR (for fraction #1 to #16) and counting the number of cells infected with HCV-like particle detected by immunofluorecense (for fraction #3 to #14) as described in Materials and Methods, respectively. In brief, each fraction were diluted with 1x PBS and HCV-like particles were collected by ultracentrifugation, then pellets were suspended in culturing medium and used for infection. (**b**) HCV-like particle collected from infectious (**Fig. 2a**, filled arrowhead) and HCV RNA (**Fig. 2a**, open arrowhead) peaks were collected by ultracentrifugation and subjected to non-reducing SDS-PAGE and detected by immunoblot against core. (**c**) HCV-like particle collected from fraction #8 to #13 (**a**) were subjected to non-reducing SDS-PAGE in the presence (+) or absence (-) of 5 mM N-ethylemaleimide (NEM) and analyzed by immunoblotting against the core. Data are representative of two (**a,** infectivity of fractions) or three independent experiments.

**Figure 3.** The core complex is formed at the LD and ER. (**a**) The LD fraction and whole-cell lysate (WCL) were collected from JFH1$^{E2FL}$ RNA–transfected HuH-7 cells

665 on day 5 post-transfection. Immunoblot analysis of the LD marker adipose
666 differentiation-related protein (ADRP) and the ER marker calnexin in the LD fraction
667 (upper panel). Immunoblot analysis of core in the LD fraction treated with or without 50
668 mM DTT (lower panel). (**b**) Immunoblot analysis of core protein in the MMF and WCL
669 collected from JFH1$^{E2FL}$-producing HuH-7 cells on day 5 post-transfection in the
670 presence or absence of 5% β-mercaptoethanol (β-ME). Data are representative of three
671 independent experiments.
672
673 **Figure 4.** The core complex consists of a core dimer. (**a**) Schematic of wild-type,
674 FLAG-tagged (FLAG-core), and Myc-tagged (Myc-core) cores. (**b**) Immunoblot
675 analysis of core in the MMF collected from HuH-7 cells transfected with combinations
676 of pcDNA3 (vector) and/or core expression plasmids (e.g., encoding core$^{WT}$,
677 FLAG-core, and Myc-core) as indicated. The experiment was performed under
678 non-reducing conditions. The lower bands represent core monomer (marked with a
679 bracket on the right). The white arrowheads indicate bands corresponding to dbd-core.
680 The black arrowheads indicate the positions of the intermediately sized core complex
681 formed by core$^{WT}$ and tagged core. Data are representative of three independent
682 experiments.

683

684 **Figure 5.** The core dimer is formed via a bond between cysteine residues at amino acid
685 position 128. (**a**) Site-directed mutagenesis of $JFH1^{E2FL}$. (**b**) Immunoblot analysis of
686 core in MMFs collected from HuH-7 cells under non-reducing condition three days
687 after transfection with $JFH1^{E2FL}$ (WT), $JFH1^{C128A}$ (C128A), $JFH1^{C184A}$ (C184A), or
688 $JFH1^{C128A}$ (C128/184A) RNA. (**c**) Infectivity of culture medium collected and
689 concentrated on day 5 post-transfection from HuH-7 cells transfected with WT, C128A,
690 C184A, or C128/184A RNA. (**d**) Real-time qRT-PCR analysis of HCV RNA titers in
691 culture medium collected at the indicated time points from HuH-7 cells transfected with
692 WT (open circles), C128A (filled circles), C184A (open squares), C128/184A (filled
693 squares) or PP/AA ($JFH1^{PP/AA}$; open triangles) RNA. (**e**) ELISAs of core levels in
694 culture medium collected at the indicated time points from HuH-7 cells transfected with
695 WT or C128A RNA. Data are representative of three independent experiments (**b, c**) or
696 are the means ± s.d. from three independent experiments (**d, e**).

697

698 **Figure 6.** Site-directed mutagenesis has no effect on HCV replication. (**a**) Real-time
699 qRT-PCR analysis of the HCV RNA titer using total cellular RNA collected at the
700 indicated time points from cells transfected with $JFH1^{E2FL}$ (WT) (open circles),

JFH1$^{C128A}$ (C128A) (filled circles), JFH1$^{C184A}$ (C184A) (open squares), JFH1$^{C128/184A}$ (C128/184A) (filled squares), or JFH1$^{PP/AA}$ (PP/AA) (open triangles) RNA. (**b**) Immunoblot analysis of NS5A and GAPDH in whole cell lysate collected from cells transfected with WT, C128A, C184A or C128/184A RNA at day 3 post-transfection. (**c**) Confocal microscopy of the subcellular localization of the LD (green), core (blue), NS5A (red), and nucleus (DAPI) (grey) in WT- and C128A core-expressing cells on day 3 post-transfection. Scale bar indicates 10 μm. (**d**) An RNA–protein binding precipitation assay was performed with *in vitro* translated core$^{WT}$ and core$^{C128A}$ using poly-U agarose as the resin. "+RNase" and "-RNase" indicate samples with and without RNase treatment, respectively, as described in the Materials and Methods. "input" indicates 1/40 of the amount of translated product used in this assay. Data represent the means ± s.d. from three independent experiments (**a**) or are representative of three independent experiments (**b-d**).

**Figure 7.** JFH1$^{C128A}$ core inhibits JFH1$^{E2FL}$ particle assembly. A competitive inhibitory assay was performed with JFH1$^{E2FL}$ (WT) and JFH1$^{C128A}$ (C128A). (**a**) Real-time qRT-PCR analysis of the HCV RNA titer in HuH-7 cell culture medium three days after the cells were transfected with the indicated ratio of WT and C128A RNA. (**b**)

719 Infectivity of culture medium collected from HuH-7 cells that had been transfected with
720 the indicated ratio of WT and C128A RNA was analyzed as described in the Materials
721 and Methods. Data represent the means ± s.d. from three independent experiments (**a**) or
722 are representative of three independent experiments (**b**).
723
724 **Figure 8.** The nucleocapsid-like particle of JFH1$^{E2FL}$ is assembled with the C-terminal
725 region of core on the outer surface. (**a**) Immunoblot analysis of core in JFH1$^{E2FL}$
726 particles collected from sucrose density gradient fractions with high HCV RNA titers
727 (particle) (**Fig. 2a,** fraction #8 to #13). Fractions were treated with 10 μg/ml trypsin at
728 37°C for 15 min in the presence or absence of 1% NP-40 (right panel). As a positive
729 control, whole cell lysate (WCL) prepared from JFH1$^{E2FL}$ RNA–transfected HuH-7 cells
730 in lysis buffer was treated with 10 μg/ml trypsin at 37°C for 15 min (left panel). (**b**)
731 Immunoblot analysis of core in JFH1$^{E2FL}$ particles collected from sucrose density
732 gradient fractions with high HCV RNA titers. Fractions were treated with the indicated
733 concentrations of trypsin at 37°C for 10 min in the presence of 1% NP-40. Open and
734 filled arrows indicate the positions of dbd-core and the trypsin-digested fragment,
735 respectively. Data are representative of three independent experiments.

**Supplementary Figure 1.** JFH1$^{E2FL}$ core protein. Map of the reported functional regions of the core protein from residues 1 to 191 is shown as indicated in figure. The white arrowheads indicate signal peptidase (SP) and proposed signal peptide peptidase (SPP) cleavage site by Okamoto et al. (37). The filled arrowheads represents potential trypsin cleavage sites. Cystein residues of the core are indicated by arrows.

**Supplementary Figure 2.** Core complexes from various HCV strains. Immunoblot analysis of core from pellets containing HCV virus particles collected following ultracentrifugation of the concentrated culture medium from JFH1$^{E2FL}$, JFH1$^{AAA99}$, J6/JFH1, or J6/JFH1$^{AAA99}$ RNA–transfected HuH-7 or HuH7.5 cells under non-reducing conditions. Data are representative of three independent experiments.

**Supplementary Figure 3.** Analysis of core complex in microsomal membrane fractions (MMF) of core expressing cells. (**a**) MMF of HuH-7 cells transfected with pcDNA3 (vector), pcDNA3-core$^{WT}$ (core$^{WT}$), or pcDNA3-C-E1/25 (C-E1/25), bearing full length core and the N-terminal 25 amino acid sequence of E1, were subjected to non-reducing ((-) β-ME) and reducing ((+) β-ME) SDS-PAGE and analyzed by immunoblotting against core. Open arrowheads indicate the non-specific bands observed in MMF samples in reducing condition which positions are close to the core dimers detected in non-reducing condition. (**b**) Immunoblot analysis of core in the MMF collected from

HuH-7 cells transfected with pcDNA3 (vector) and/or core expression plasmids (core191, FLAG-core, and Myc-core) as indicated. Samples were treated with or without 5% β-mercaptoethanol (β-ME). Filled arrowheads indicate the positions of the intermediate core complexes formed by $core^{WT}$ and tagged core. Data are representative of two (**a**) or three (**b**) independent experiments.

**Supplementary Figure 4.** Site-directed mutagenesis of amino-acid position 127 or 129 had no effect on HCV replication or the production of HCV particles. (**a**) Immunoblot analysis of core in microsomal membrane fractions collected on day 3 post-transfection from cells transfected with $JFH1^{E2FL}$ (WT), $JFH1^{T127A}$ (T127A), or $JFH1^{G129A}$ RNA. Samples were treated with or without 5% β-mercaptoethanol (β-ME). (**b**, **c**) Real-time qRT-PCR analysis of HCV RNA titers in total cellular RNA (**b**) or culture medium (**c**) collected on day 5 post-transfection. Data are representative of three independent experiments (**a**) or are the means ± s.d. from three independent experiments (**b**, **c**).

**Supplementary Figure 5.** Analysis of core C128S mutant. (**a**) Real-time qRT-PCR analysis of HCV RNA titers in culture medium collected at the indicated time points from HuH-7 cells transfected with $JFH1^{E2FL}$ (WT, open circles) or $JFH1^{C128S}$ (C128S, filled circles) RNA. (**b**) Real-time qRT-PCR analysis of the HCV RNA titer using total

775 cellular RNA collected at the indicated time points from cells transfected with WT
776 (open circles) or (C128S) (filled circles). (**c**) Immunoblot analysis of core in microsomal
777 membrane fraction collected on day 3 post-transfection from cells transfected with
778 JFH1$^{E2FL}$ (WT) or JFH1$^{C128S}$ RNA (C128S). (**d**) Infectivity of culture medium collected
779 and concentrated on day 5 post-transfection from HuH-7 cells transfected with WT or
780 C128S RNA. (**e**) Confocal microscopy of the subcellular localization of the LD (green),
781 core (blue), NS5A (red), and nucleus (DAPI) (grey) in cells transfected with JFH1$^{E2FL}$
782 (WT) or JFH1$^{C128S}$ RNA (C128S) on day 3 post-transfection. Data are the means ± s.d.
783 from three independent experiments (**c**, **b**) or are representative of three independent
784 experiments (**c, d, e**).
785
786 **Supplementary Figure 6.** Subcellular localization of HCV proteins. Confocal
787 microscopy of the subcellular localizations of the lipid droplet (LD), core, NS5A, and
788 the nucleus (DAPI) three days post-transfection with JFH1$^{C184A}$ (C184A) or
789 JFH1$^{C128/184A}$ (C128/184A). Scale bar indicates 10 μm. Data are representative of three
790 independent experiments.
791
792 **Supplementary Figure 7.** Transfection of various amounts of HCV RNA had no

793 effect on HCV replication. (**a**) Real-time qRT-PCR analysis of the HCV RNA titer in
794 total cellular RNA collected on day 3 post-transfection from HuH-7 cells transfected
795 with the indicated RNA ratio of JFH1$^{E2FL}$ (WT) or JFH1$^{C128A}$ (C128A) RNA. (**b**)
796 Real-time qRT-PCR analysis of the HCV RNA titer in total cellular RNA (open bars) or
797 culture medium (filled circles) collected on day 3 post-transfection from HuH-7 cells
798 transfected with the indicated amount of JFH1$^{E2FL}$ RNA. (**d**)Real-time qRT-PCR
799 analysis of the HCV RNA titer in total cellular RNA (open bars) or culture medium
800 (filled circles) collected on day 3 post-transfection from HuH-7 cells transfected with
801 the indicated ratio of WT and JFH1$^{dc3}$ (dc3) RNA. (**c, e**) The infectivity of culture
802 medium collected from HuH-7 cells transfected with the indicated amount of JFH1$^{E2FL}$
803 RNA (**c**) and culture medium collected from HuH-7 cells transfected with the indicated
804 ratio of WT and JFH1$^{dc3}$ (dc3) RNA (**e**) were analyzed as described in the Materials and
805 Methods. Data are the means ± s.d. from three independent experiments (**a, b, d**) or are
806 representative of three independent experiments (**c, e**).
807
808 **Supplementary Table.** The sets of primers used to amplify the target genes, template
809 plasmids used in the PCRs, restriction sites, and plasmids into which the amplified DNA
810 fragments were inserted are shown.

*Figures and Legends for:*

# A DISULFIDE-BONDED DIMER OF THE CORE PROTEIN OF HEPATITIS C VIRUS IS IMPORTANT FOR VIRUS-LIKE PARTICLE PRODUCTION

**Yukihiro Kushima,[1, 2] Takaji Wakita,[3] Makoto Hijikata[1, 2]**

1. **Department of Viral Oncology, Institute for Virus Research, Kyoto University, Kyoto 606-8507, Japan**
2. **Graduate School of Biostudies, Kyoto University, Kyoto 606-8507, Japan**
3. **Department of Virology II, National Institute of Infectious Diseases, Tokyo 162-8640, Japan**

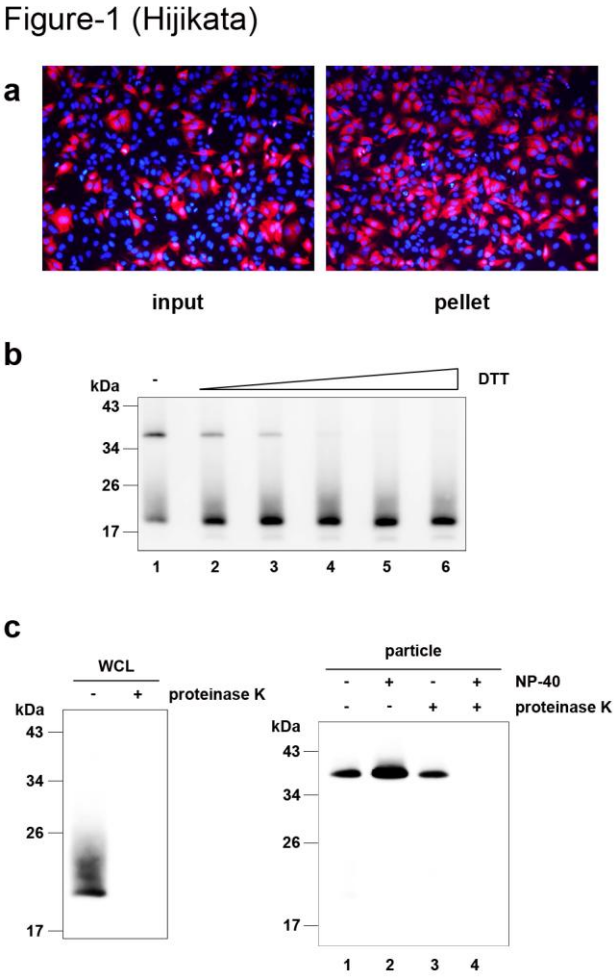


**Figure 1.** The HCV-like particle consists of a core complex formed by a disulfide bond. (**a**) The infectivity of the pellet fraction collected from concentrated culture medium from JFH1$^{E2FL}$ RNA–transfected HuH-7 cells was analyzed as described in the Materials and Methods. "input" represents the same volume of concentrated culture medium used to pellet the virus-like particles. (**b**) Immunoblot analysis of the core in pellets containing JFH1$^{E2FL}$ virus particles treated with various levels of DTT (lanes 1, 2, 3, 4, 5 and 6 represent 0, 1.56, 3.13, 6.25, 12.5 and 25 mM, respectively). (**c**) Immunoblot analysis of core in JFH1$^{E2FL}$ particles collected from sucrose density gradient fractions with high HCV RNA titers (particle) (**Fig. 2a,** fraction #8 to #13) and treated with 5 μg/ml proteinase K at 3°C for 15 min in the presence or absence of 1% NP-40 (right panel). As a positive control, whole-cell lysate (WCL) prepared from JFH1$^{E2FL}$ RNA–transfected HuH-7 cells in lysis buffer was treated with 5 μg/ml proteinase K at 37°C for 15 min (left panel). Data are representative of three independent experiments.

**Figure-2 (Hijikata)**

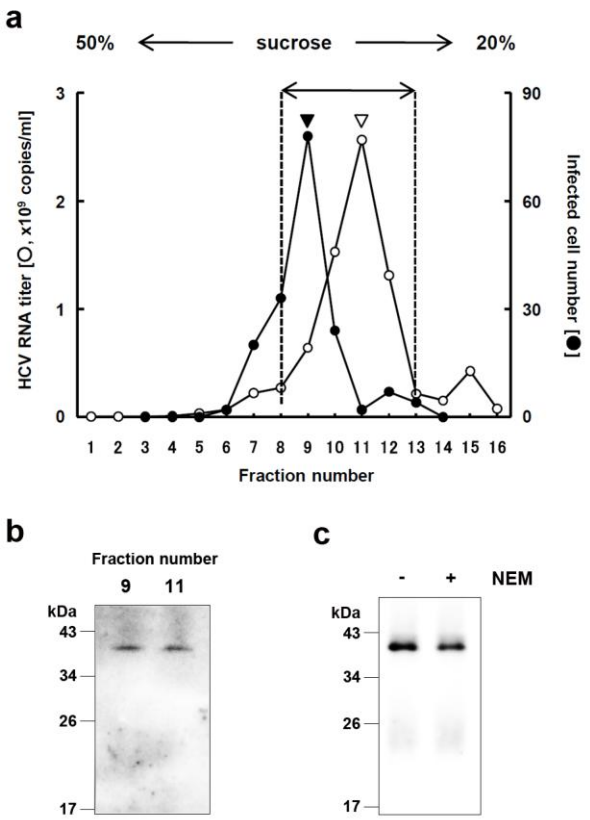


**Figure 2.** HCV nucleocapsid-like particle consists of core complex. (**a**) HCV RNA titer in culture medium separated on a 20-50% sucrose density gradient. Concentrated culture medium from JFH1$^{E2FL}$ RNA–transfected HuH-7 cells were treated with RNase and separated on a 20-50% sucrose density gradient. Fractions were obtained from the bottom to the top of the tube (#1 to #16). The HCV RNA titer and infectivity of each fraction were analyzed by real-time qRT-PCR (for fraction #1 to #16) and counting the number of cells infected with HCV-like particle detected by immunofluorecense (for fraction #3 to #14) as described in Materials and Methods, respectively. In brief, each fraction were diluted with 1x PBS and HCV-like particles were collected by ultracentrifugation, then pellets were suspended in culturing medium and used for infection. (**b**) HCV-like particle collected from infectious (**Fig. 2a**, filled arrowhead) and HCV RNA (**Fig. 2a**, open arrowhead) peaks were collected by ultracentrifugation and subjected to non-reducing SDS-PAGE and detected by immunoblot against core. (**c**) HCV-like particle collected from fraction #8 to #13 (**a**) were subjected to non-reducing SDS-PAGE in the presence (+) or absence (-) of 5 mM N-ethylemaleimide (NEM) and analyzed by immunoblotting against the core. Data are representative of two (**a,** infectivity of fractions) or three independent experiments.

Figure-3 (Hijikata)

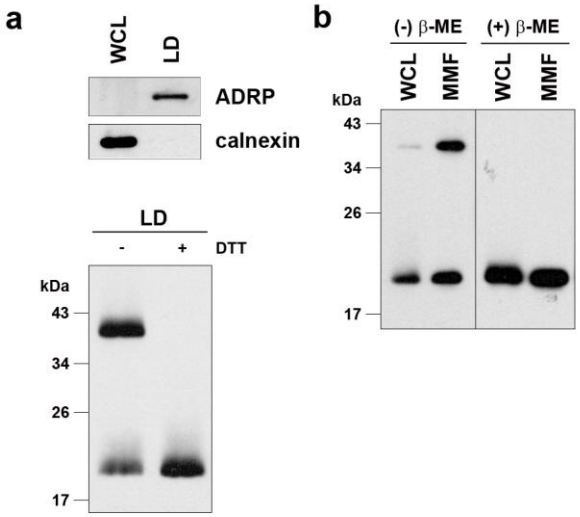


**Figure 3.** The core complex is formed at the LD and ER. (**a**) The LD fraction and whole-cell lysate (WCL) were collected from JFH1$^{E2FL}$ RNA–transfected HuH-7 cells on day 5 post-transfection. Immunoblot analysis of the LD marker adipose differentiation-related protein (ADRP) and the ER marker calnexin in the LD fraction (upper panel). Immunoblot analysis of core in the LD fraction treated with or without 50 mM DTT (lower panel). (**b**) Immunoblot analysis of core protein in the MMF and WCL collected from JFH1$^{E2FL}$-producing HuH-7 cells on day 5 post-transfection in the presence or absence of 5% β-mercaptoethanol (β-ME). Data are representative of three independent experiments.

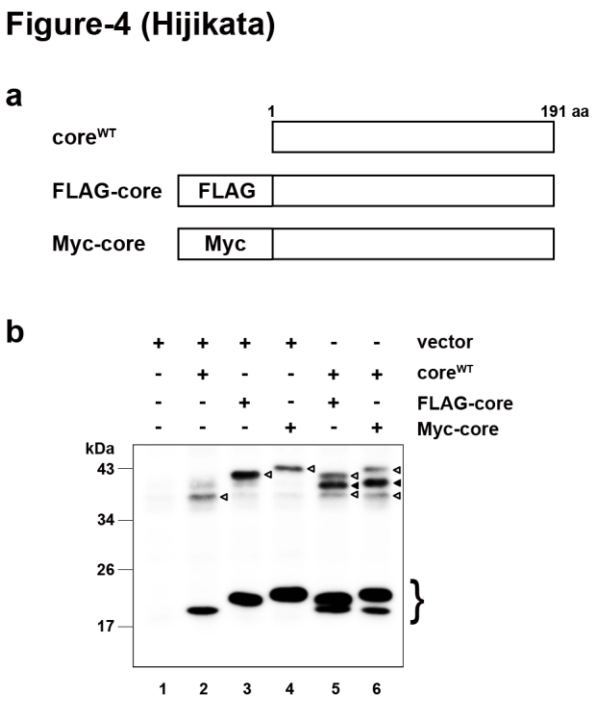


**Figure 4.** The core complex consists of a core dimer. (**a**) Schematic of wild-type, FLAG-tagged (FLAG-core), and Myc-tagged (Myc-core) cores. (**b**) Immunoblot analysis of core in the MMF collected from HuH-7 cells transfected with combinations of pcDNA3 (vector) and/or core expression plasmids (e.g., encoding core$^{WT}$, FLAG-core, and Myc-core) as indicated. The experiment was performed under non-reducing conditions. The lower bands represent core monomer (marked with a bracket on the right). The white arrowheads indicate bands corresponding to dbd-core. The black arrowheads indicate the positions of the intermediately sized core complex formed by core$^{WT}$ and tagged core. Data are representative of three independent experiments.

Figure-5 (Hijikata)

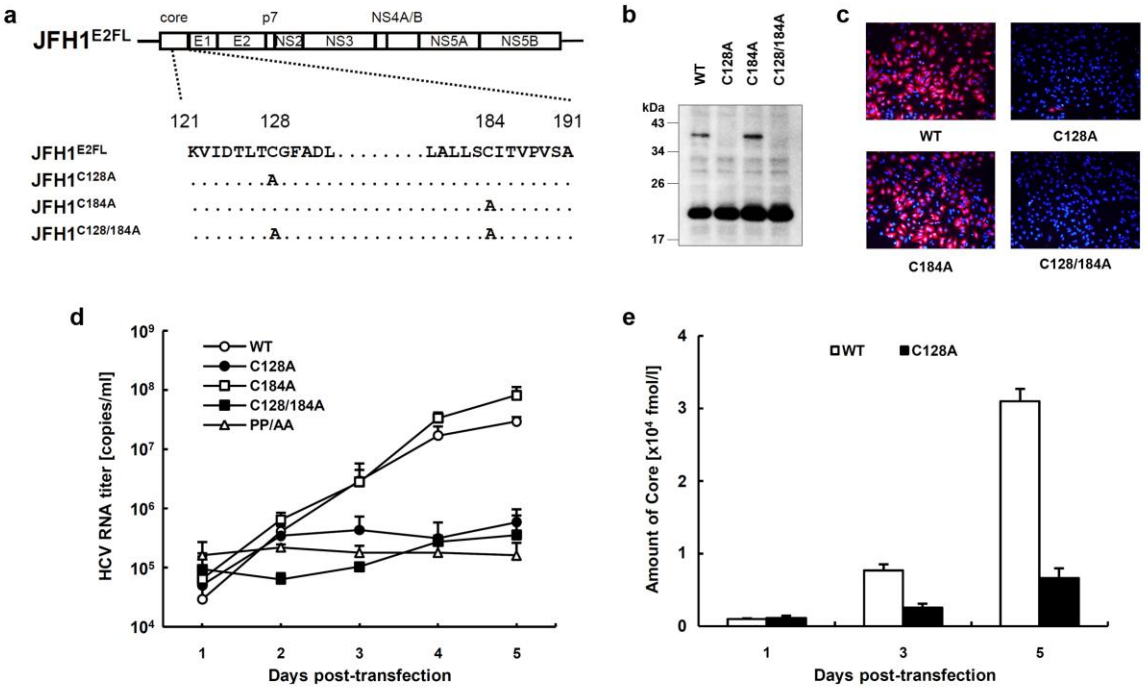


**Figure 5.** The core dimer is formed via a bond between cysteine residues at amino acid position 128. (**a**) Site-directed mutagenesis of JFH1$^{E2FL}$. (**b**) Immunoblot analysis of core in MMFs collected from HuH-7 cells under non-reducing condition three days after transfection with JFH1$^{E2FL}$ (WT), JFH1$^{C128A}$ (C128A), JFH1$^{C184A}$ (C184A), or JFH1$^{C128A}$ (C128/184A) RNA. (**c**) Infectivity of culture medium collected and concentrated on day 5 post-transfection from HuH-7 cells transfected with WT, C128A, C184A, or C128/184A RNA. (**d**) Real-time qRT-PCR analysis of HCV RNA titers in culture medium collected at the indicated time points from HuH-7 cells transfected with WT (open circles), C128A (filled circles), C184A (open squares), C128/184A (filled squares) or PP/AA (JFH1$^{PP/AA}$; open triangles) RNA. (**e**) ELISAs of core levels in culture medium collected at the indicated time points from HuH-7 cells transfected with WT or C128A RNA. Data are representative of three independent experiments (**b, c**) or are the means ± s.d. from three independent experiments (**d, e**).

Figure-6 (Hijikata)

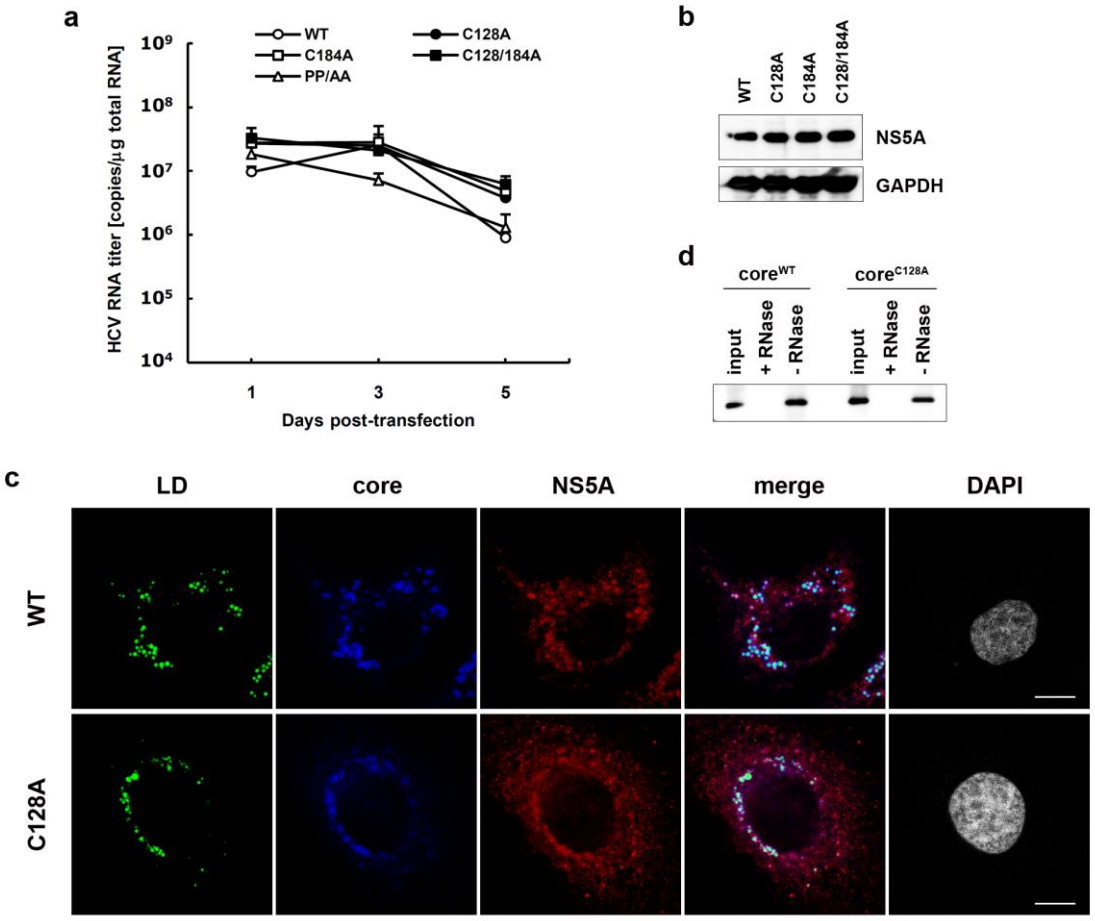


**Figure 6.** Site-directed mutagenesis has no effect on HCV replication. (**a**) Real-time qRT-PCR analysis of the HCV RNA titer using total cellular RNA collected at the indicated time points from cells transfected with JFH1$^{E2FL}$ (WT) (open circles), JFH1$^{C128A}$ (C128A) (filled circles), JFH1$^{C184A}$ (C184A) (open squares), JFH1$^{C128/184A}$ (C128/184A) (filled squares), or JFH1$^{PP/AA}$ (PP/AA) (open triangles) RNA. (**b**) Immunoblot analysis of NS5A and GAPDH in whole cell lysate collected from cells transfected with WT, C128A, C184A or C128/184A RNA at day 3 post-transfection. (**c**) Confocal microscopy of the subcellular localization of the LD (green), core (blue), NS5A (red), and nucleus (DAPI) (grey) in WT- and C128A core-expressing cells on day 3 post-transfection. Scale bar indicates 10 μm. (**d**) An RNA–protein binding precipitation assay was performed with *in vitro* translated core$^{WT}$ and core$^{C128A}$ using poly-U agarose as the resin. "+RNase" and "-RNase" indicate samples with and without RNase treatment, respectively, as described in the Materials and Methods. "input" indicates 1/40 of the amount of translated product used in this assay. Data represent the means ± s.d. from three independent experiments (**a**) or are representative of three independent experiments (**b-d**).

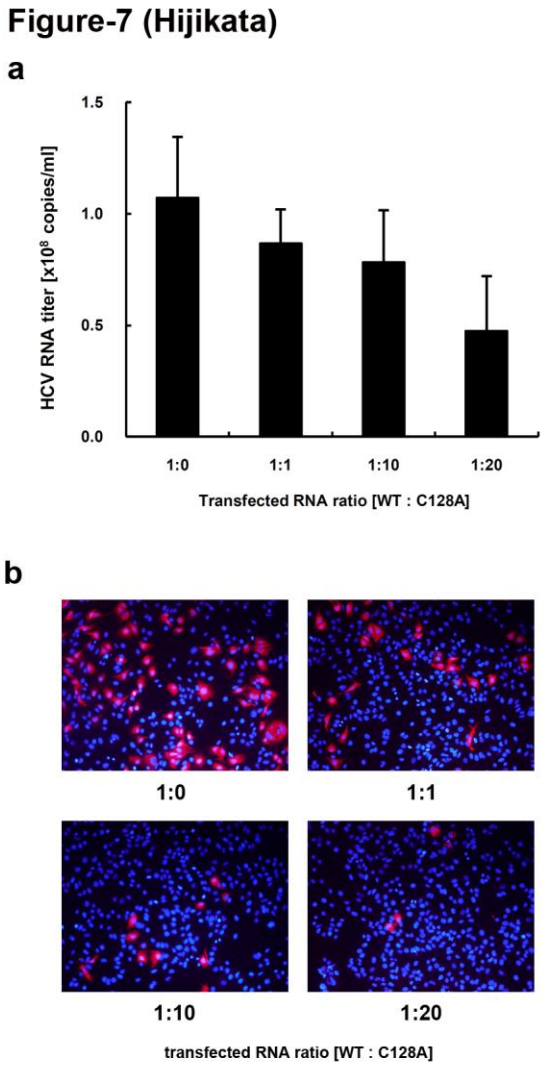


**Figure 7.** JFH1$^{C128A}$ core inhibits JFH1$^{E2FL}$ particle assembly. A competitive inhibitory assay was performed with JFH1$^{E2FL}$ (WT) and JFH1$^{C128A}$ (C128A). (**a**) Real-time qRT-PCR analysis of the HCV RNA titer in HuH-7 cell culture medium three days after the cells were transfected with the indicated ratio of WT and C128A RNA. (**b**) Infectivity of culture medium collected from HuH-7 cells that had been transfected with the indicated ratio of WT and C128A RNA was analyzed as described in the Materials and Methods. Data represent the means ± s.d. from three independent experiments (**a**) or are representative of three independent experiments (**b**).

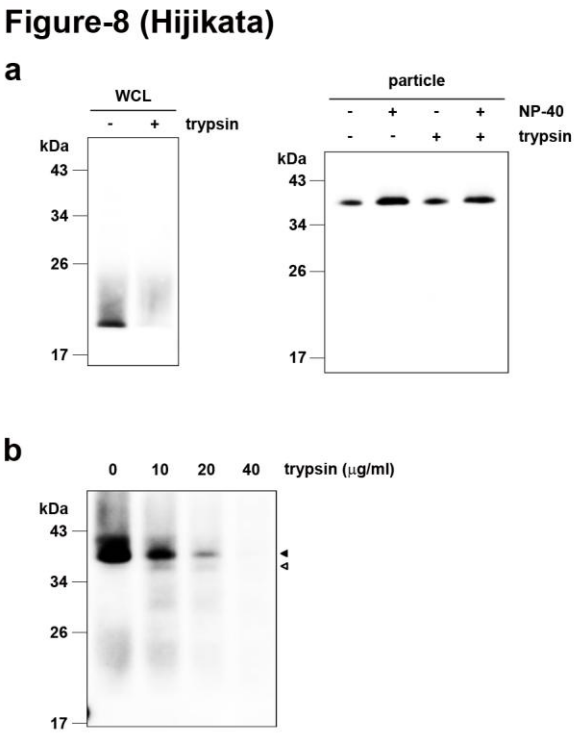


**Figure 8.** The nucleocapsid-like particle of JFH1$^{E2FL}$ is assembled with the C-terminal region of core on the outer surface. (**a**) Immunoblot analysis of core in JFH1$^{E2FL}$ particles collected from sucrose density gradient fractions with high HCV RNA titers (particle) (**Fig. 2a,** fraction #8 to #13). Fractions were treated with 10 μg/ml trypsin at 37°C for 15 min in the presence or absence of 1% NP-40 (right panel). As a positive control, whole cell lysate (WCL) prepared from JFH1$^{E2FL}$ RNA–transfected HuH-7 cells in lysis buffer was treated with 10 μg/ml trypsin at 37°C for 15 min (left panel). (**b**) Immunoblot analysis of core in JFH1$^{E2FL}$ particles collected from sucrose density gradient fractions with high HCV RNA titers. Fractions were treated with the indicated concentrations of trypsin at 37°C for 10 min in the presence of 1% NP-40. Open and filled arrows indicate the positions of dbd-core and the trypsin-digested fragment, respectively. Data are representative of three independent experiments.

*Supplementary imformation for:*

# A DISULFIDE-BONDED DIMER OF THE CORE PROTEIN OF HEPATITIS C VIRUS IS IMPORTANT FOR VIRUS-LIKE PARTICLE PRODUCTION

**Yukihiro Kushima,[1, 2] Takaji Wakita,[3] Makoto Hijikata[1, 2]**

1. **Department of Viral Oncology, Institute for Virus Research, Kyoto University, Kyoto 606-8507, Japan**
2. **Graduate School of Biostudies, Kyoto University, Kyoto 606-8507, Japan**
3. **Department of Virology II, National Institute of Infectious Diseases, Tokyo 162-8640, Japan**

## Supplementary Figures and legends

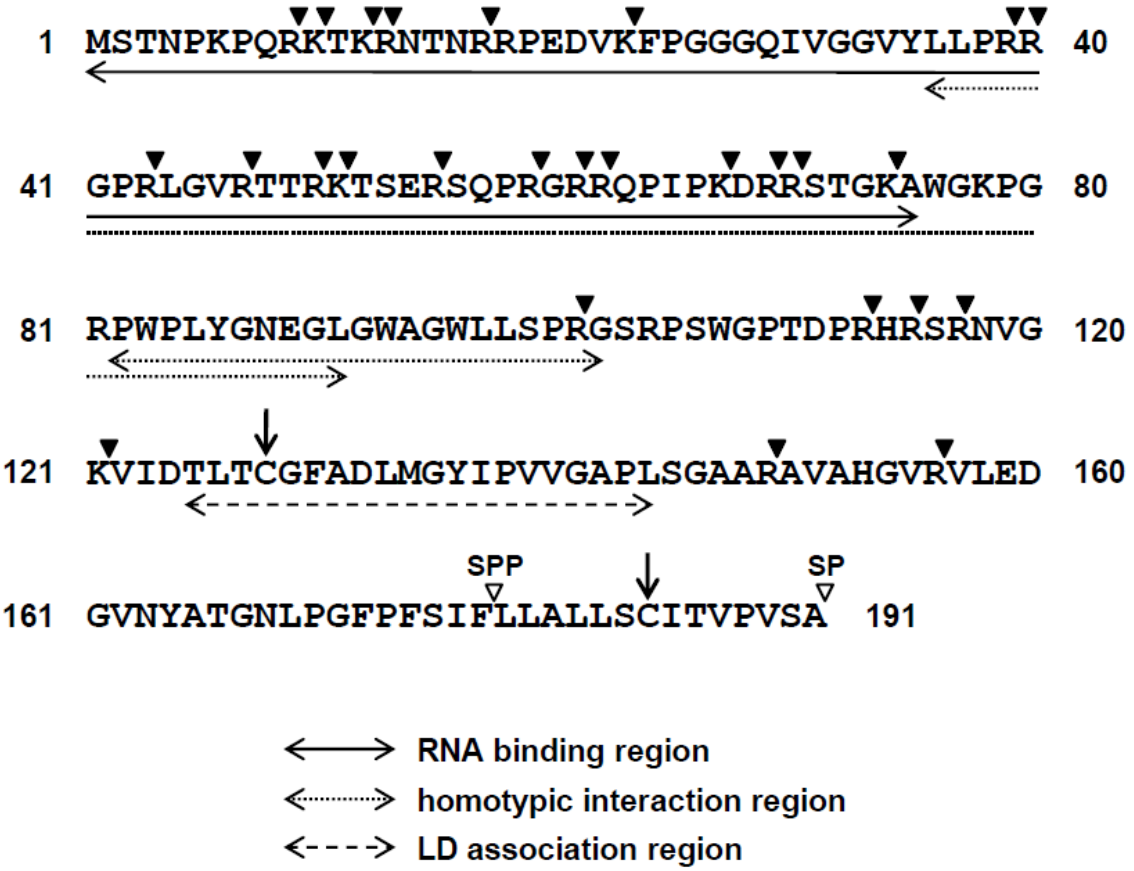


**Supplementary Figure 1.** JFH1$^{E2FL}$ core protein. Map of the reported functional regions of the core protein from residues 1 to 191 is shown as indicated in figure. The white arrowheads indicate signal peptidase (SP) and proposed signal peptide peptidase (SPP) cleavage site by Okamoto et al. (37). The filled arrowheads represents potential trypsin cleavage sites. Cystein residues of the core are indicated by arrows.

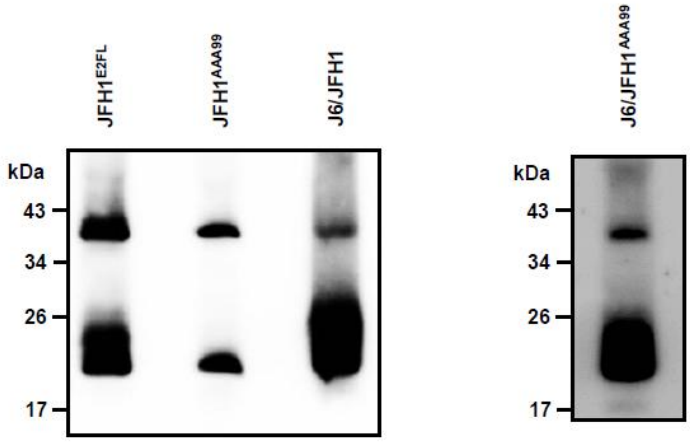


**Supplementary Figure 2.** Core complexes from various HCV strains. Immunoblot analysis of core from pellets containing HCV virus particles collected following ultracentrifugation of the concentrated culture medium from JFH1$^{E2FL}$, JFH1$^{AAA99}$, J6/JFH1, or J6/JFH1$^{AAA99}$ RNA–transfected HuH-7 or HuH7.5 cells under non-reducing conditions. Data are representative of three independent experiments.

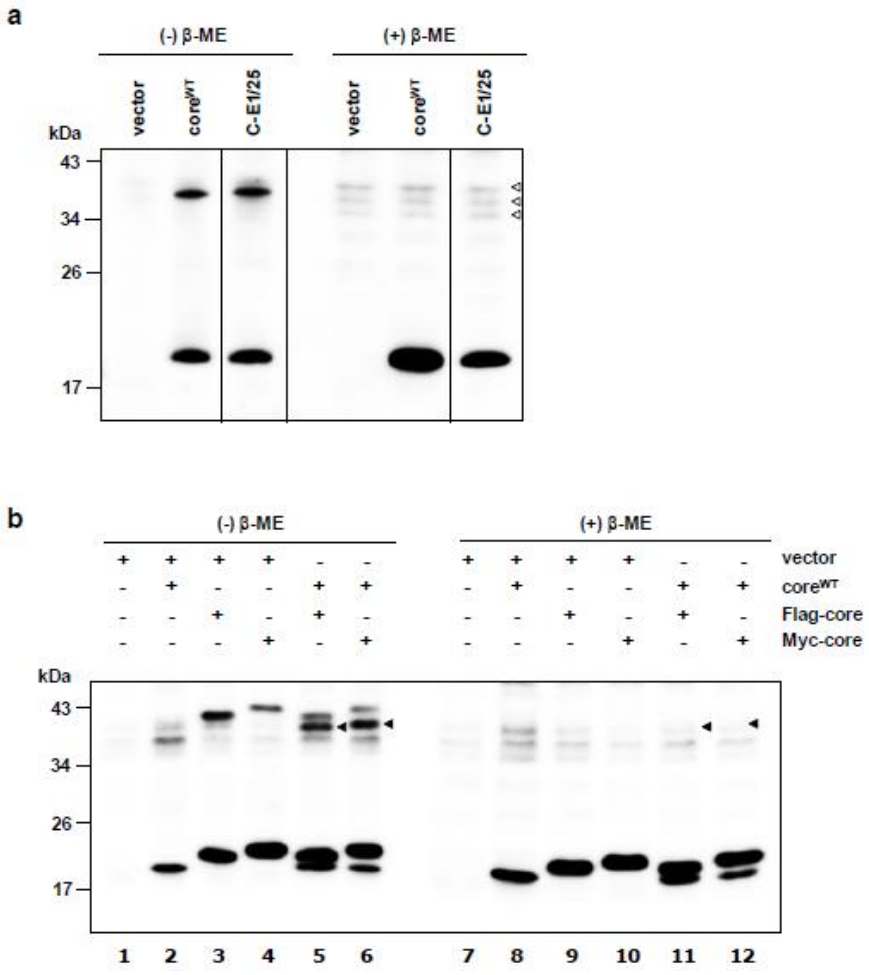


**Supplementary Figure 3.** Analysis of core complex in microsomal membrane fractions (MMF) of core expressing cells. (**a**) MMF of HuH-7 cells transfected with pcDNA3 (vector), pcDNA3-core$^{WT}$ (core$^{WT}$), or pcDNA3-C-E1/25 (C-E1/25), bearing full length core and the N-terminal 25 amino acid sequence of E1, were subjected to non-reducing ((-) β-ME) and reducing ((+) β-ME) SDS-PAGE and analyzed by immunoblotting against core. Open arrowheads indicate the non-specific bands observed in MMF samples in reducing condition which positions are close to the core dimers detected in non-reducing condition. (**b**) Immunoblot analysis of core in the MMF collected from HuH-7 cells transfected with pcDNA3 (vector) and/or core expression plasmids (core191, FLAG-core, and Myc-core) as indicated. Samples were treated with or without 5% β-mercaptoethanol (β-ME). Filled arrowheads indicate the positions of the intermediate core complexes formed by core$^{WT}$ and tagged core. Data are representative of two (**a**) or three (**b**) independent experiments.

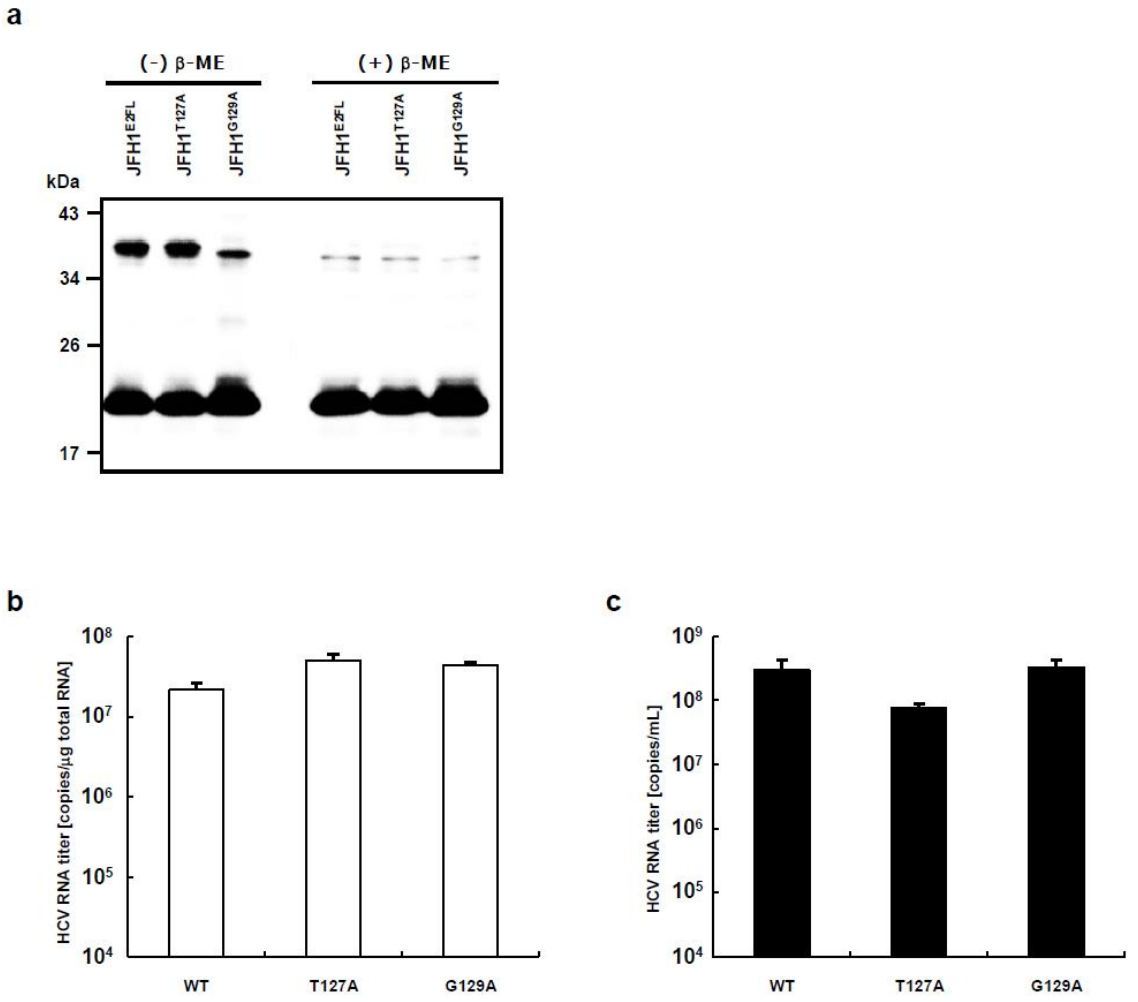


**Supplementary Figure 4.** Site-directed mutagenesis of amino-acid position 127 or 129 had no effect on HCV replication or the production of HCV particles. (**a**) Immunoblot analysis of core in microsomal membrane fractions collected on day 3 post-transfection from cells transfected with JFH1$^{E2FL}$ (WT), JFH1$^{T127A}$ (T127A), or JFH1$^{G129A}$ RNA. Samples were treated with or without 5% β-mercaptoethanol (β-ME). (**b**, **c**) Real-time qRT-PCR analysis of HCV RNA titers in total cellular RNA (**b**) or culture medium (**c**) collected on day 5 post-transfection. Data are representative of three independent experiments (**a**) or are the means ± s.d. from three independent experiments (**b**, **c**).

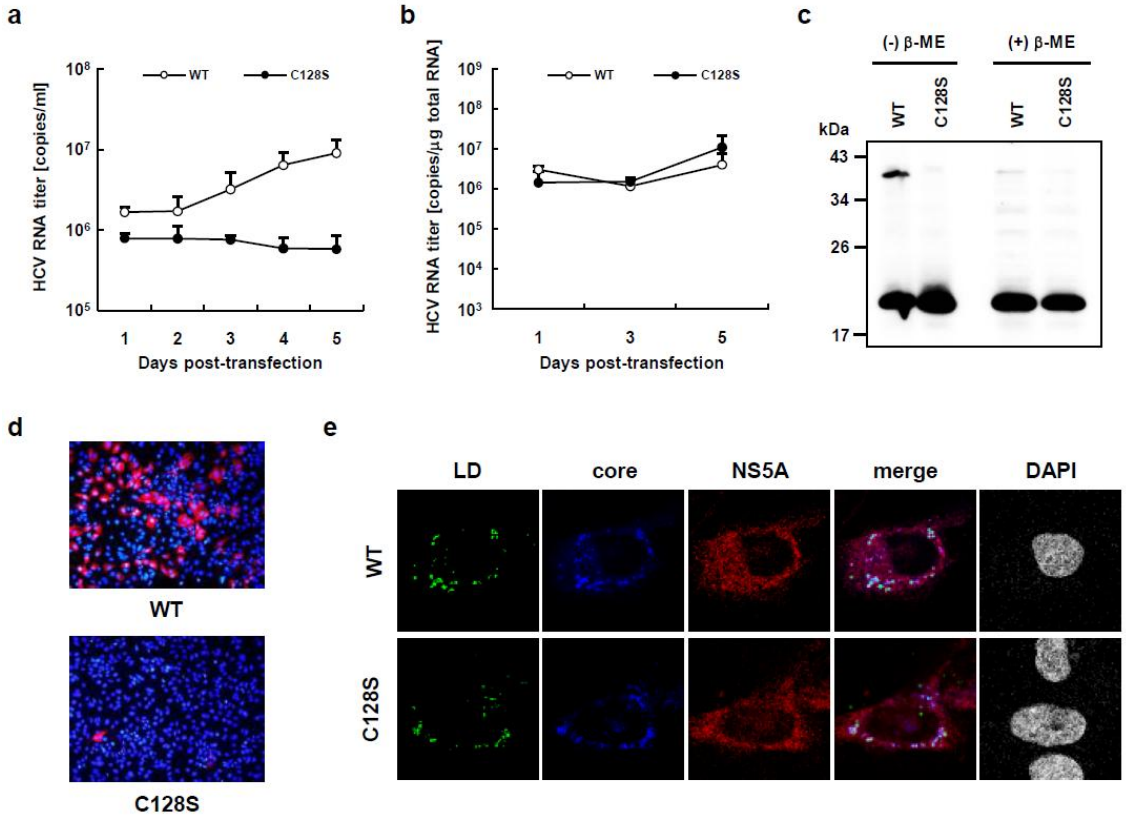


**Supplementary Figure 5.** Analysis of core C128S mutant. (**a**) Real-time qRT-PCR analysis of HCV RNA titers in culture medium collected at the indicated time points from HuH-7 cells transfected with JFH1$^{E2FL}$ (WT, open circles) or JFH1$^{C128S}$ (C128S, filled circles) RNA. (**b**) Real-time qRT-PCR analysis of the HCV RNA titer using total cellular RNA collected at the indicated time points from cells transfected with WT (open circles) or (C128S) (filled circles). (**c**) Immunoblot analysis of core in microsomal membrane fraction collected on day 3 post-transfection from cells transfected with JFH1$^{E2FL}$ (WT) or JFH1$^{C128S}$ RNA (C128S). (**d**) Infectivity of culture medium collected and concentrated on day 5 post-transfection from HuH-7 cells transfected with WT or C128S RNA. (**e**) Confocal microscopy of the subcellular localization of the LD (green), core (blue), NS5A (red), and nucleus (DAPI) (grey) in cells transfected with JFH1$^{E2FL}$ (WT) or JFH1$^{C128S}$ RNA (C128S) on day 3 post-transfection. Data are the means ± s.d. from three independent experiments (**c**, **b**) or are representative of three independent experiments (**c, d, e**).

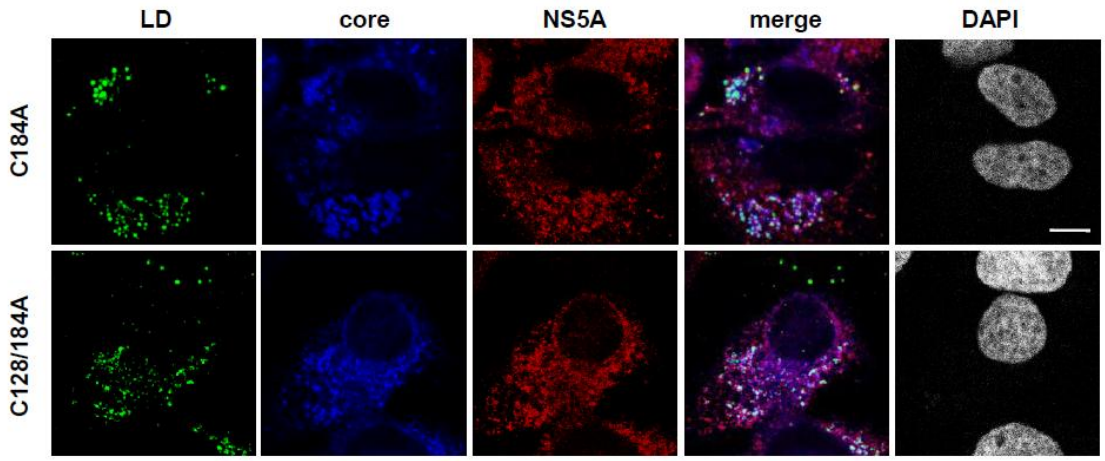


**Supplementary Figure 6.** Subcellular localization of HCV proteins. Confocal microscopy of the subcellular localizations of the lipid droplet (LD), core, NS5A, and the nucleus (DAPI) three days post-transfection with $JFH1^{C184A}$ (C184A) or $JFH1^{C128/184A}$ (C128/184A). Scale bar indicates 10 μm. Data are representative of three independent experiments.

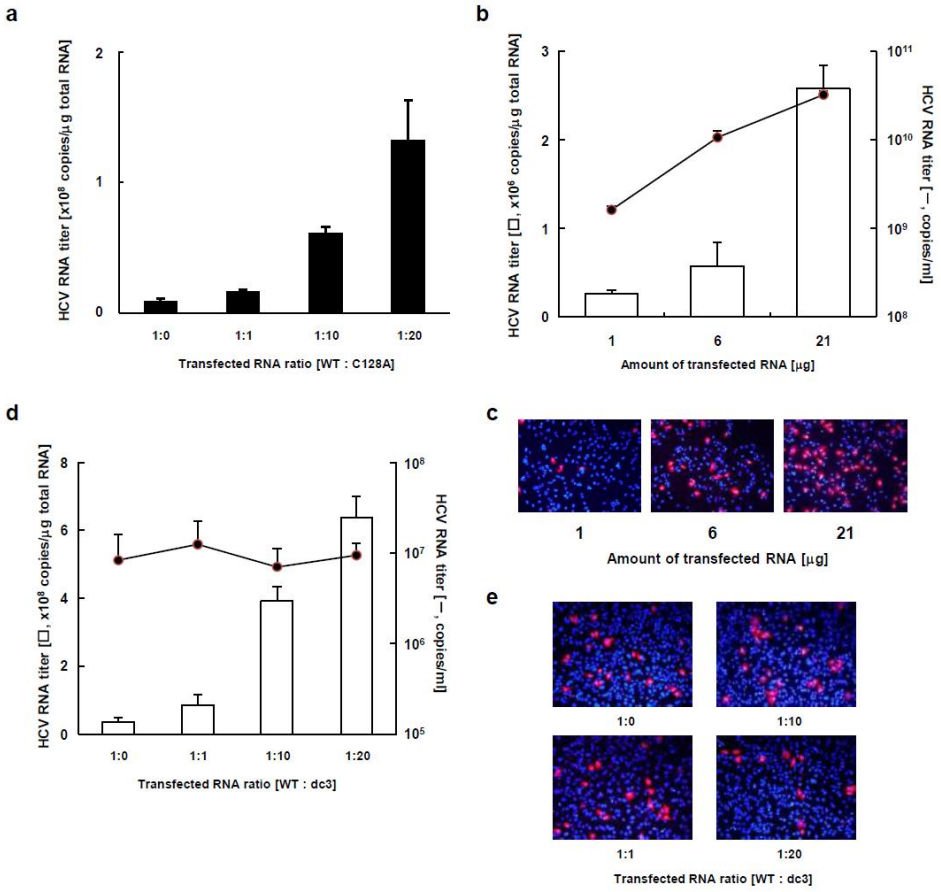


**Supplementary Figure 7.** Transfection of various amounts of HCV RNA had no effect on HCV replication. (**a**) Real-time qRT-PCR analysis of the HCV RNA titer in total cellular RNA collected on day 3 post-transfection from HuH-7 cells transfected with the indicated RNA ratio of JFH1$^{E2FL}$ (WT) or JFH1$^{C128A}$ (C128A) RNA. (**b**) Real-time qRT-PCR analysis of the HCV RNA titer in total cellular RNA (open bars) or culture medium (filled circles) collected on day 3 post-transfection from HuH-7 cells transfected with the indicated amount of JFH1$^{E2FL}$ RNA. (**d**)Real-time qRT-PCR analysis of the HCV RNA titer in total cellular RNA (open bars) or culture medium (filled circles) collected on day 3 post-transfection from HuH-7 cells transfected with the indicated ratio of WT and JFH1$^{dc3}$ (dc3) RNA. (**c, e**) The infectivity of culture medium collected from HuH-7 cells transfected with the indicated amount of JFH1$^{E2FL}$ RNA (**c**) and culture medium collected from HuH-7 cells transfected with the indicated ratio of WT and JFH1$^{dc3}$ (dc3) RNA (**e**) were analyzed as described in the Materials and Methods. Data are the means ± s.d. from three independent experiments (**a, b, d**) or are representative of three independent experiments (**c, e**).

| Plasmid name | Primer sequences (5'-3') | Template for PCR | Restriction enzyme site | Original plasmid |
|---|---|---|---|---|
| pJFH1$^{T127A}$ | CACGACGTTGTAAAACGACG | pJFH1$^{E2FL}$ | EcoRI / BsiWI | pJFH1$^{E2FL}$ |
| | ATCGACACCCTAGCGTGTGGCTT | | | |
| | ATGTCTATGATGACCTCGGG | | | |
| pJFH1$^{C128A}$ | CACGACGTTGTAAAACGACG | pJFH1$^{E2FL}$ | EcoRI / BsiWI | pJFH1$^{E2FL}$ |
| | ACCCTAACGGCTGGCTTTGCC | | | |
| | ATGTCTATGATGACCTCGGG | | | |
| pJFH1$^{C128S}$ | CACGACGTTGTAAAACGACG | pJFH1$^{E2FL}$ | EcoRI / BsiWI | pJFH1$^{E2FL}$ |
| | ACCCTAACGTCTGGCTTTGCC | | | |
| | ATGTCTATGATGACCTCGGG | | | |
| pJFH1$^{G129A}$ | CACGACGTTGTAAAACGACG | pJFH1$^{E2FL}$ | EcoRI / BsiWI | pJFH1$^{E2FL}$ |
| | ACCCTAACGTGTGCCTTTGCCGACCTC | | | |
| | ATGTCTATGATGACCTCGGG | | | |
| pJFH1$^{C184A}$ | CACGACGTTGTAAAACGACG | pJFH1$^{E2FL}$ | EcoRI / BsiWI | pJFH1$^{E2FL}$ |
| | CCTGTTGTCCGCCATCACCGTTC | | | |
| | ATGTCTATGATGACCTCGGG | | | |
| pJFH1$^{C128/184A}$ | CACGACGTTGTAAAACGACG | pJFH1$^{C184A}$ | EcoRI / BsiWI | pJFH1$^{E2FL}$ |
| | ACCCTAACGGCTGGCTTTGCC | | | |
| | ATGTCTATGATGACCTCGGG | | | |
| pcDNA3-C-E1/25 | tgataAAGCTTCACCATGAGCACAAATCC | pJFH1$^{E2FL}$ | HindIII / EcoRI | pcDNA3 |
| | taataGAATTCTCACGGGGACGTGGAGAACCG | | | |
| pcDNA3-FLAG-core | tgataAAGCTTACCATGGACTACAAGGATGAC GATGACAAGATGAGCACAAATCCTAAAC | pJFH1$^{E2FL}$ | HindIII / EcoRI | pcDNA3 |
| | taataGAATTCTCAAGCAGAGACCGGAACG | | | |
| pcDNA3-Myc-core | tgataAAGCTTACCATGGAACAAAAACTCATC TCAGAAGAGGATCTGATGAGCACAAATCC TAAAC | pJFH1$^{E2FL}$ | HindIII / EcoRI | pcDNA3 |
| | taataGAATTCTCAAGCAGAGACCGGAACG | | | |
| pcDNA3-core$^{C128A}$ | tgataAAGCTTCACCATGAGCACAAATCC | pJFH1$^{C128A}$ | HindIII / EcoRI | pcDNA3 |
| | taataGAATTCTCAAGCAGAGACCGGAACG | | | |

**Supplementary Table.** The sets of primers used to amplify the target genes, template plasmids used in the PCRs, restriction sites, and plasmids into which the amplified DNA fragments were inserted are shown.